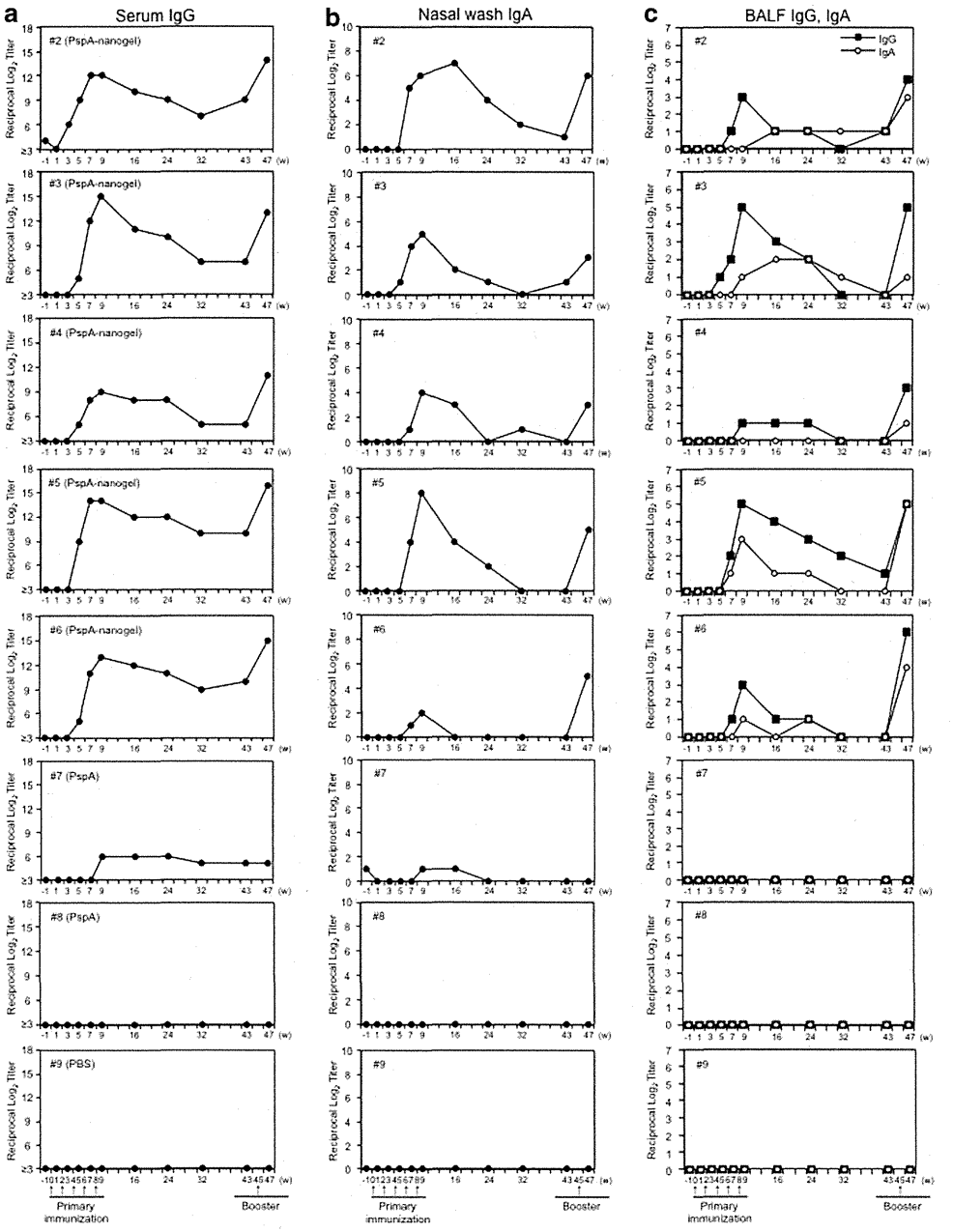

Figure 2 Nasal immunization with PspA-nanogel induced PspA-specific Ab responses in macaques. Each cynomolgus macaque was nasally immunized with PspA-nanogel (macaques #2-#6), PspA alone (#7 and #8), or PBS only (#9) at the times indicated with arrows. Serum, nasal wash, and BALF were collected, and the levels of PspA-specific serum IgG (**a**), nasal wash IgA (**b**), and BALF IgG and IgA (**c**) were determined by ELISA. BALF, bronchoalveolar lavage fluid.

after the initial PspA-nanogel immunization (**Figure 2a–c**). Of importance, a nasal booster induced higher levels of PspA-specific IgA Ab responses in BALF of two macaques (#5 and #6) than those observed after the primary immunization (**Figure 2c**).

These findings suggest that memory-type PspA-specific Ab responses are induced in nonhuman primates after nasal vaccination with PspA-nanogel. PspA-nanogel is therefore a promising nasal vaccine candidate that can induce long-lasting antigen-specific systemic and mucosal immunity and can elicit nasal booster activity in nonhuman primates.

Nasal immunization with PspA-nanogel induces neutralizing Abs against *S. pneumoniae* in macaques

To investigate whether the nasal PspA-nanogel vaccine induced neutralizing Abs, we examined whether PspA-specific serum Abs from macaques nasally immunized with PspA-nanogel would passively protect against pneumococcal infection. CBA/N mice were injected intraperitoneally with diluted pooled sera of macaques nasally immunized with PspA-nanogel, PspA alone, or PBS only. When all groups of mice were challenged with *S. pneumoniae* Xen10 or 3JYP2670 strain via the intravenous route, mice passively immunized with sera

from macaques nasally immunized with PspA-nanogel were fully protected for at least 2 weeks (**Figure 3a,b**). In contrast, mice that received sera from macaques given nasal PspA alone or PBS only died within 5 days post-challenge (**Figure 3a,b**). These results demonstrated that protective immunity with subtype cross-reactivity was induced by nasal PspA-nanogel vaccination.

Nasal immunization with PspA-nanogel induces Th2 and Th17 responses in macaques

As macaques nasally immunized with PspA-nanogel showed high IgG/IgA Ab responses, we next determined the levels of cytokine production in $CD4^+$ T cells isolated from blood of the macaques. The macaques nasally immunized with PspA-nanogel showed increased levels of IL-4 and IL-17 production by $CD4^+$ T cells when compared with macaques given PspA alone or PBS only (**Figure 4b,c**). However, essentially identical levels of IFN-γ were produced by $CD4^+$ T cells isolated from macaques nasally immunized with PspA-nanogel, PspA alone, or PBS only (**Figure 4a**). Furthermore, we showed that nasal immunization with PspA-nanogel induced PspA-specific IgG1 Ab responses, which is the hallmark of the Th2-type immune response (**Figure 4d**). These results indicated that the nasal PspA-nanogel vaccine could induce Th2 and Th17 cytokine responses.

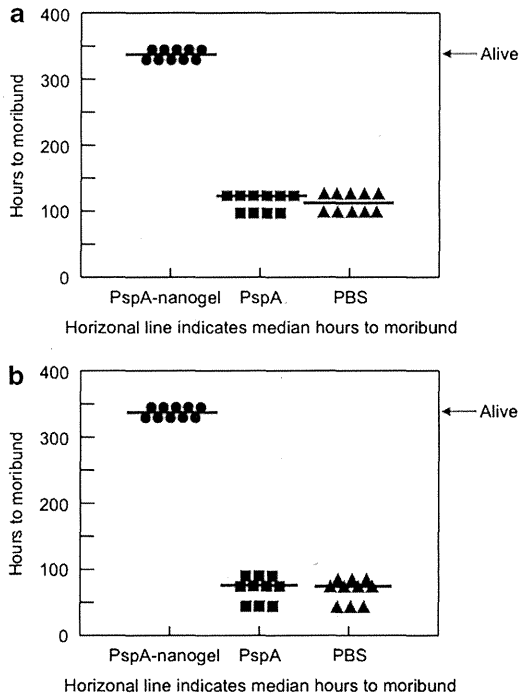

Figure 3 Neutralizing Abs induced by nasal immunization with PspA-nanogel. Serum from each of the macaques was collected 1 week after the final primary nasal immunization with PspA-nanogel, PspA alone, or PBS only. CBA/N mice (10 mice per group) were passively transferred with 100 μl of diluted (1:20) pooled sera via i.p. route. Four hours later, mice were injected i.v. with 1.5×10^4 c.f.u. *S. pneumoniae* Xen 10 (**a**) or 1×10^3 c.f.u. *S. pneumoniae* 3JYP2670 strain (**b**). The mice were monitored daily for mortality. Each line represents the median survival time. c.f.u., colony-forming unit; i.p., intraperitoneal; i.v., intravenous.

Nasal immunization with PspA-nanogel increases the expression levels of miRNAs in serum and respiratory tract tissues in macaques

To examine the roles of miRNA in the induction of PspA-specific immunity, we performed miRNA microarray analysis to identify immunologically associated differences in serum miRNA profiles between pre-immunized and post-boosted macaques (data not shown). We selected some immunologically relevant miRNAs, namely miR-181a, miR-326, miR-155, miR-17, miR-18a, miR-20a, and miR-92a, the levels of which were upregulated in post-booster serum samples compared with pre-immunized serum samples. To further confirm whether these immunologically relevant miRNAs were upregulated or downregulated in post-booster serum samples compared with pre-immunized or pre-booster serum samples, we performed quantitative RT–PCR of them. Expression levels of miR-326, Th17-cell differentiation-related miRNA, and miR-181a, T-cell and B-cell differentiation-related miRNA, were significantly increased in the sera of macaques given a nasal booster dose of PspA-nanogel when compared with control macaques as pre-immunization (**Figure 5a**). The levels of the two miRNAs were also shown significantly higher in the respiratory tract tissues, including nasal tissues and lungs, of macaques given a booster dose of PspA-nanogel than the levels in the corresponding tissues of control macaques given PspA alone or PBS only that was set at 1 (**Figure 5b,c**). Furthermore, we analyzed the expression level of Ets-1, which is a known negative regulator of Th17 cells and is the functional target of miR-326. We detected a significant decrease in the expression level of Ets-1 mRNA in the lungs of macaques given a booster dose of PspA-nanogel compared with those of control macaques given PspA alone or PBS only (**Figure 5c**). These results suggest that these miRNAs have important roles in T-cell and B-cell differentiation and in Th17 cytokine responses after nasal immunization with PspA-nanogel in macaques.

DISCUSSION

By using a nonhuman primate system, we demonstrated that the nasal PspA-nanogel vaccine did not accumulate in the CNS and effectively induced both mucosal and systemic immunity associated with protection against pneumococcal infection. To our knowledge, this study is the first to report the safety and effectiveness of a nasal PspA vaccine in macaques; therefore, our results provide a concrete rationale for testing our nanogel-based PspA vaccine in humans.

The nanogel itself is non-immunogenic material, and a cancer-specific protein (e.g., Her 2) complexed with a neutral CHP nanogel produced by means of good manufacturing practices (GMP) has been used as an injectable cancer vaccine in clinical research.[28] In our previous study, nasal immunization with CHP-nanogel containing PspA induces effective antigen-specific immune responses in mice[21] but not in macaques (data not shown); therefore, in the present study, we developed a cCHP nanogel containing 20 amino groups per 100 glucose units to improve antigen delivery to the nasal

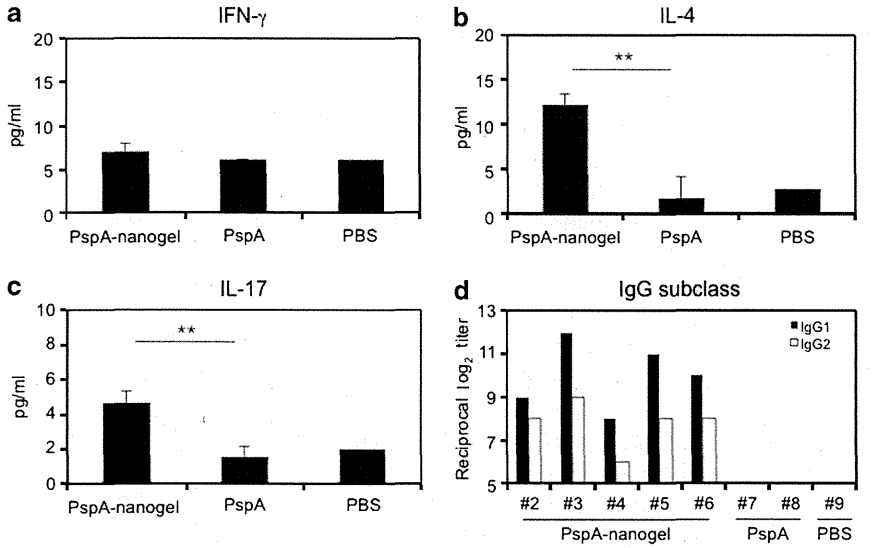

Figure 4 PspA-nanogel immunization produced $CD4^+$ Th2- and Th17-type cytokine responses. $CD4^+$ T cells were separated from the PBMCs 1 week after the booster. Purified $CD4^+$ T cells were cultured with irradiated APCs and 5 μg ml^{-1} of PspA with anti-CD28 and CD49d antibodies for 5 days. The levels of the cytokines, IFN-γ (**a**), IL-4 (**b**), and IL-17A (**c**) in the supernatants were measured. This experiment was repeated in triplicate. Values are shown as the means ± s.d. in each experimental group. $^{**}P < 0.01$ compared between PspA-nanogel and PspA/PBS groups. (**d**) Serum from macaques was collected 1 week after the final primary nasal immunization with PspA-nanogel (#2-#6), PspA alone (#7, #8), or PBS only (#9). Expression levels of PspA-specific serum IgG subclass Abs were determined by using ELISA. APCs, antigen-presenting cells; IFN, interferon; IL, interleukin; PBMC, peripheral blood mononuclear cells.

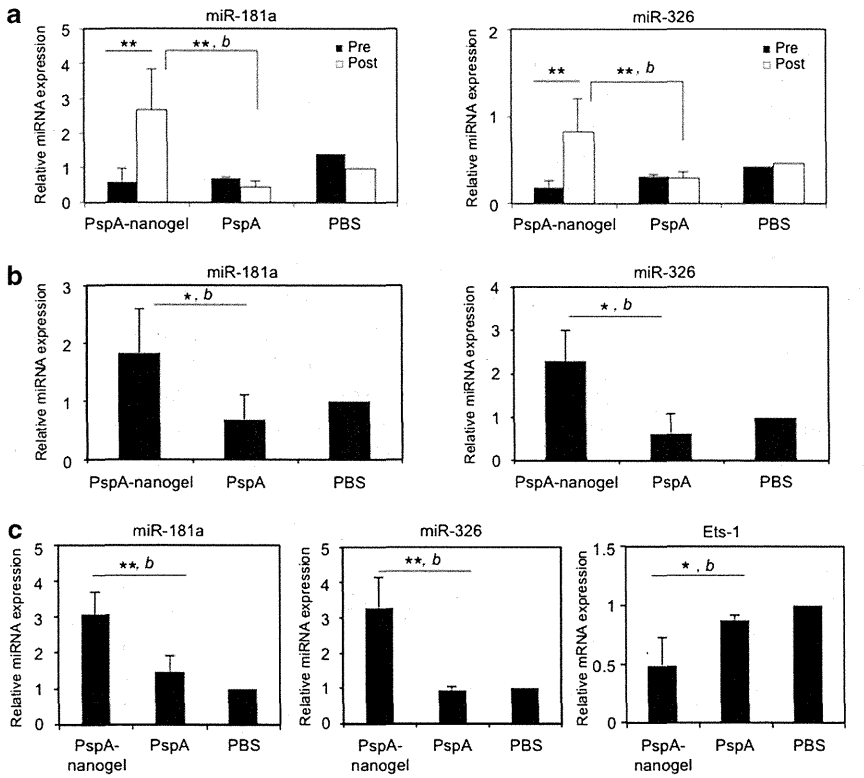

Figure 5 MiRNA expression levels in sera (**a**), nasal tissues (**b**), and lung tissues (**c**) of macaques nasally immunized with PspA-nanogel, PspA alone, or PBS only. Expression levels of the indicated miRNA and Ets-1 mRNA were analyzed by quantitative RT–PCR and normalized to the levels of miR-16 and β-actin, respectively. Values are shown as the means ± s.d. in each experimental group. $^{*}P < 0.05$, $^{**}P < 0.01$ when compared between pre-immunization and post-booster groups. *b*, Compared between PspA-nanogel and PspA/PBS groups in post-booster macaques. MiRNA, microRNA; Pre, pre-immunized serum; Post, post-booster serum.

epithelium layer of macaques. We confirmed the perfect complex formation and the size of PspA-nanogel complex using fluorescence response energy transfer (FRET) analysis and dynamic light scattering (DLS): the cCHP nanogel spontaneously formed nanoparticles after the incorporation of PspA (**Supplementary Figure S1a,b**).[18,19] In addition, consistent with its positive zeta-potential (**Supplementary Figure S1b**), *in vivo* PET and MRI imaging in macaques clearly showed that nasally administered cCHP nanogel carrying [^{18}F]-labeled PspA was more effectively delivered to and continuously retained at the nasal mucosa of macaques when compared with nasally delivered [^{18}F]-PspA alone. These results indicated that the new cationic group-modified cCHP nanogel would be able to efficiently deliver the vaccine antigen to the anionic nasal epithelium following nasal administration in macaques. Indeed, our previous mouse model studies have shown that the nanogel–antigen complex is retained and taken up into the epithelium by endocytosis, where the antigen is released from the nanogel in the epithelium by strong chaperone-like activity. The antigen is then released from the nasal epithelium by exocytosis and subsequently taken up effectively by DCs.[19,21]

Recent studies of nasal vaccines have raised concerns about the deposition and accumulation of candidate vaccine antigens or co-administered mucosal adjuvants in the CNS through direct transport from the nasal cavity to the cerebrum via the olfactory pathways.[29,30] It has also been reported that many peptides and proteins bypass the blood–brain and blood–cerebrospinal fluid barriers to reach the CNS following nasal administration in humans.[31] In this study, we showed that there was no deposition or accumulation of [^{18}F]-PspA in the CNS over a period of up to 6 h after nasal administration of [^{18}F]-PspA-nanogel in macaques. As we validated the detection limit of our PET system for [^{18}F]-protein by direct tissue counting in our previous study,[32] [^{18}F] radioactivity in this study was <0.05 SUV in the cerebrum and olfactory bulbs of the macaques. Therefore, our current results demonstrated that the cCHP delivered nasal PspA vaccine did not reach the CNS of macaques, even though the olfactory epithelium in the nasal cavity is connected to the CNS,[31] thereby confirming the safety of the vaccine in higher mammals.

The mucosal immune system consists of both inductive and effector sites and has a key role in the induction and regulation of dynamic immune responses, including the Th2-type-cell-dependent SIgA response, the mucosal cytotoxic T-cell response, and the Th17-cell-mediated immune regulatory response.[33] In general, IgA in mucosal tissue is thought to have an important role in protection against respiratory pathogens including *S. pneumoniae*.[15–17] In this study, we showed that the PspA-nanogel vaccine also induced mucosal antigen-specific mucosal IgA and systemic IgG Ab responses in the macaques. Especially, serum and BALF IgG, the main isotype of antibody in the lower respiratory compartment, have key roles in survival against lethal challenge with *S. pneumoniae*.[34] Importantly, the macaque IgG antibodies to PspA, which are supported by CD4$^+$ Th2-type cytokine IL-4, possessed protective activity against *S. pneumoniae*. When mice were systemically challenged with *S. pneumoniae* Xen10 or 3JYP2670 after mice passively immunized with macaques' sera containing PspA-specific Abs, they showed complete protection. Our findings indicate that this protection is clearly due to antibody-mediated immunity to PspA. These results are consistent with those of a previous study in mice showing that nasal vaccination induces functional CD4$^+$ Th2-type cytokine-mediated IgG Ab responses, which are sufficient to provide appropriate protection in the absence of Th1-type cytokine responses.[16] In addition, induction of the BALF IgG responses is essential, as antigen-specific IgG is known to exert protection at the alveolar level following to promote phagocytosis and prevents local dissemination of the pneumococcus and its passage into the blood.[34] These results demonstrated that the nasal PspA-nanogel vaccine effectively induced PspA-specific serum IgG with protective activity in addition to SIgA Ab immune responses in nonhuman primates.

Recent studies have shown that specific miRNAs are involved in T-cell and B-cell development, differentiation, and regulatory functions.[24,35] Especially, miR-181a is highly expressed in mature T cells and has an important effect on the positive and negative selection process by controlling the strength of TCR signaling during thymic development of T cells for subsequent Th1 and Th2 differentiation, indicating that miR-181a modulates T-cell development.[36] In this study, the expression levels of miR-181a in the serum and respiratory tract tissues, including nasal tissues and lungs, were significantly higher in macaques nasally immunized with PspA-nanogel than in those given PspA alone or PBS only, indicating that miRNAs are implicated in adaptive immunity by controlling the activation of T cells after nasal immunization with PspA-nanogel in nonhuman primates. Furthermore, we showed that the levels of miR-155, which is required for the production of high-affinity IgG1 Abs, were increased in PspA-nanogel-immunized macaques (**Supplementary Figure S2a–c**).[37] These results indicated that PspA-nanogel-induced Th2 cytokine response was mediated through the increased expression of miR-155.

MiR-181a is also highly expressed in B cells and within bone marrow cells and germinal center B cells, where it promotes the differentiation of hematopoietic stem cells into B cells.[24,38] To explore the roles of other miRNAs that are also highly expressed in germinal center B cells and are essential for adult B-cell development, we examined the expression of the miR-17-92 cluster.[39,40] The miR-17-92 cluster regulates follicular helper T cell (Tfh cell) differentiation by controlling the migration of CD4$^+$ T cells into B-cell follicles,[41] suggesting that these miRNAs have an important role in the production of antigen-specific SIgA Ab. We found here that not only miR-181a expression but also miR-17-92 cluster expression was markedly increased in the nasal tissues of nasally PspA-nanogel-immunized macaques (**Supplementary Figure S3**). Detection of these mucosal IgA-associated miRNAs in the nasal tissues of nasally PspA-nanogel-immunized macaques

indicates that they contribute substantially to the production of mucosal IgA.

It is well known that IL-17-mediated $CD4^+$ T cells are important for the generation of resistance to mucosal colonization by respiratory pathogens including *S. pneumoniae* in humans and mice.[42,43] Trzcinski *et al.*[44] demonstrated that antigen-specific $CD4^+$ T-cell immunity is sufficient to protect against nasopharyngeal colonization by *S. pneumoniae* in mice. Studies in mice indicated that pulmonary Th17 responses are associated with migration of B cells into airways and with the promotion of polymeric Ig receptor (pIgR) expression by airway epithelial cells.[45] In addition, Th17 cells are a crucial subset of Th cells responsible for inducing the switch of germinal center B cells toward T-cell-dependent IgA production.[46] Furthermore, IL-17-secreting memory Th17 cells increased by human pneumococcal carriage have been reported to enhance innate cellular immunity against pneumococcal challenge.[47] Therefore, it is important to determine whether antigen-specific $CD4^+$ Th17 responses are induced by nasal immunization with PspA-nanogel in nonhuman primates. Recent studies have shown that miR-326-mediated Th17 upregulation might provide the host with a potentiating effect to recruit functional immune cells to local effector sites in response to pathogen attack.[48] We found here that nasal immunization with PspA-nanogel in macaques prompted the generation of IL-17-producing cells in the peripheral blood $CD4^+$ T cells. Furthermore, our miRNA analysis showed that expression levels of Th17-associated miR-326 in the serum, nasal tissues, and lungs were significantly increased and that the expression level of Ets-1 mRNA, a negative regulator of Th17 differentiation, was decreased in the lungs of the PspA-nanogel-vaccinated macaques. Therefore, our finding that miR-326-associated IL-17-secreting $CD4^+$ T cells were generated after nasal vaccination with PspA-nanogel suggests that it would be useful for the development of safe and efficacious nasal vaccines against pneumonia and that serum miR-326 could be used as a biomarker to evaluate vaccine efficacy.

In summary, we demonstrated for the first time that a nasal PspA-nanogel vaccine induced both humoral and cellular immune responses in macaques. These results were supported by increased expression levels of miR-181a and miR-326, which are candidate miRNA biomarkers for induction of mucosal immunity. In addition, a [^{18}F]-PspA PET study showed long-term retention of PspA in the nasal cavity and no deposition of PspA in the CNS of the macaques. Taken together, these findings demonstrate the efficacy and safety of nasal PspA-nanogel vaccine in nonhuman primates. We conclude that the nasal PspA-nanogel vaccine should now be studied in humans for its possible use as an adjuvant-free nasal vaccine.

METHODS

Animals. Eight female naive cynomolgus macaques (*Macaca fascicularis*, 5 years old, ~3 kg) were used for the immunization study and were maintained at the Tsukuba Primate Research Center for Medical Science at the National Institute of Biomedical Innovation (NIBIO, Ibaraki, Japan). In a separate experiment, one naive male rhesus macaque (*M. mulatta*, 5–6 years old, ~5 kg) was used for the PET imaging study, which was conducted at PET Center of Hamamatsu Photonics K.K. To assay antibody protection against *S. pneumoniae*, female CBA/N mice (6 weeks old) were purchased from Japan SLC (Shizuoka, Japan). All experiments were performed in accordance with the Guidelines for Use and Care of Experimental Animals, and the protocol was approved by the Animal Committee of NIBIO, Hamamatsu Photonics K.K., and The University of Tokyo.

Recombinant PspA. Recombinant PspA of *S. pneumoniae* Rx1, which belongs to PspA family 1 and clade 2, was prepared as described previously, with slight modification.[10] In brief, the plasmid encoding PspA/Rx1 (GenBank accession no. M74122; amino acids 1 through 302, pUAB055) was used to transform *E. coli* BL21 (DE3) cells. To construct pUAB055, a 909-bp fragment of PspA from a pneumococcal strain Rx1 was cloned into the pET20b vector (Novagen, Darmstadt, Germany) between the *NcoI* and *XhoI* sites. Recombinant PspA/Rx1 contains the first 302 amino acids of mature PspA plus six poly-histidines added through protein fusion at the C-terminal end. The sonicated cell supernatant was loaded onto a DEAE-Sepharose column (BD Healthcare, Piscataway, NJ) and a nickel affinity column (Qiagen, Valencia, CA), followed by gel filtration on a Sephadex G-100 column (BD Healthcare).

Preparation of recombinant PspA–nanogel complex. The cCHP nanogel (~40 nm size) generated from cationic type of cholesteryl group-bearing pullulan was used for all experiments. This cCHP nanogel contained 20 amino groups per 100 glucose units. The PspA-cCHP nanogel complex for each immunization was prepared by mixing 25 μg of PspA with cCHP at a 1:5 molecular ratio (59.45 μl per macaque) and incubating for 1 h at 46 °C. FRET was determined with an FP-6500 fluorescence spectrometer (JASCO, Tokyo, Japan) with FITC-conjugated PspA and TRITC-conjugated cCHP nanogel.[18,19] The hydrodynamic radius was assessed by means of DLS and the zeta-potential of cCHP carrying or not carrying, PspA was determined with a Zetasizer Nano ZS instrument (Malvern Instruments, Worcestershire, UK).[18,19]

Nasal immunization and sample collection. Cynomolgus macaques were nasally immunized five times at 2-week intervals with PspA-nanogel under ketamine anesthesia. For the control group, macaques were nasally administered with 25 μg of PspA alone, or PBS only. Eight months after the final immunization, the macaques were nasally boosted with the same amount of PspA-nanogel, PspA alone or PBS only. Serum, nasal wash, and BALF were collected before primary immunization, 1 week after each immunization, 2, 4, 6, and 8 months after the final immunization, and 2 weeks after receipt of the booster.

PspA-specific ELISA. The antigen-specific Ab responses were analyzed by ELISA as described previously.[21] In brief, 96-well plates were coated with 1 μg ml^{-1} PspA in PBS overnight at 4 °C. After blocking with 1 % BSA in PBS-Tween, twofold serial dilutions of samples were added and incubated for 2 h at room temperature (RT). After washing of the samples, horseradish peroxidise (HRP)-conjugated goat anti-monkey IgG (Nordic Immunological Laboratory, Tilburg, The Netherlands) or HRP-conjugated goat anti-monkey IgA (Cortex Biochem, San Leandro, CA) diluted 1:1,000 was added and incubated for 2 h at room temperature. For subclass analysis, sheep anti-human IgG1 and IgG2 (Binding Site, Birmingham, UK) and HRP-conjugated donkey anti-sheep IgG (Rockland, Limerick, PA) were used for detection. The reaction was developed with the use of TMB Microwell Peroxidase Substrate System (XPL, Gaithersburg, MD). End-point titers were expressed as the reciprocal $\log_2$ of the last dilution that gave an OD_{450} of 0.1 greater than the negative control.

Passive protection of mice with macaques' serum samples. Pooled serum samples from macaques nasally immunized with PspA-

nanogel, PspA alone, or PBS only were diluted with PBS (1:20) and injected into CBA/N mice via the intraperitoneal route (100 µl per mouse). Four hours later, all groups of mice were challenged with 1.5×10^4 CFU *S. pneumoniae* Xen 10 ($LD_{50} = 2 \times 10^2$ CFU for CBA/N mice) or 1×10^3 CFU *S. pneumoniae* 3JYP2670 strain ($LD_{50} = 7 \times 10^2$ CFU for CBA/N mice) via the intravenous route and observed daily for death for 2 weeks. Information about *S. pneumoniae* strains is available in **Supplementary Materials**.

PspA-specific CD4$^+$ T-cell responses. One week after the macaques had received the booster, lymphocytes were isolated from the peripheral blood by using Ficoll-Paque PLUS (GE Healthcare, Little Chalfont, UK). We could not separate the lymphocytes from two macaques (#3 and #6). After washing of the samples, CD4$^+$ T cells were purified by using CD4 microbeads and magnetic cell sorting (AutoMACS; Miltenyi Biotec, Auburn, CA). The cells remaining after the removal of CD4$^+$ and CD8$^+$ T cells (by using CD8 microbeads) were used as antigen-presenting cells after irradiation at 3,000 rad. Purified CD4$^+$ T cells (1×10^5 cells/well) and antigen-presenting cells (0.5×10^5 cells/well) were resuspended in RPMI 1640 (Nacalai Tesque, Kyoto, Japan) supplemented with 10 % FCS and penicillin-streptomycin (Gibco, Carlsbad, CA), and were cultured in 24-well plates for 5 days in the presence of 5 µg ml^{-1} PspA with anti-CD28 (clone CD28.2) and CD49d (clone 9F10) antibodies (0.5 µg ml^{-1} each; eBioscience, San Diego, CA) at 37 °C in 5% CO_2. Supernatants were then collected. The concentrations of the cytokines, IFN-γ, IL-4, and IL-17 in the supernatants were measured with a Monkey Singleplex Bead Kit (Invitrogen, Carlsbad, CA) and Bio-Plex 200 (Bio-Rad, Hercules, CA).

Synthesis of [^{18}F]-PspA. Purified PspA was radiolabeled by conjugation with *N*-succinimidyl-4-[^{18}F]fluorobenzoate ([^{18}F]SFB), which reacts with free amino groups, including the N-terminal and ε-Lys amino groups in the protein, as described previously.[19,32] The product was purified by gel-permeation chromatography (Superose 12, PBS, 1 ml min^{-1}), and the radioactive peak that eluted at 12.7 min was collected. The 615 MBq [^{18}F]-PspA was obtained at 150 min from the end of bombardment. The radiochemical purity and the decay-corrected radiochemical yield were 100 and 2.95%, respectively. The specific activity was 1,798 to 4,045 MBq mg^{-1} protein.

PET/MRI imaging in rhesus macaques. Because the half-life of [^{18}F] is only 110 min, we used the same naive macaque for nasal [^{18}F]-PspA-nanogel or [^{18}F]-PspA-PBS administration with a 1-week interval between administrations. After nasal administration of 50 MBq per 700 µl of [^{18}F]-PspA-nanogel or [^{18}F]-PspA-PBS (350 µl in each nostril), the macaque's head was tilted back for 10 min and then scanned in an upright position. PET scans were conducted for 345 min with frames of 25 × 3 min, followed by 27 × 10 min, with the use of a high-resolution animal PET scanner (SHR-7700; Hamamatsu Photonics, Shizuoka, Japan). MRI images were recorded with Signa Excite HDxt (3T; GE Healthcare) to identify the cerebrum regions.

Image data analysis. PET data were analyzed by means of the PMOD software package (PMOD Technologies, Zurich, Switzerland). Each PET image was superimposed on the corresponding MRI data to identify the volume of interest. Time-activity curves (TACs) of PET/MRI images were expressed as % remaining dose.

MiRNA expression levels in serum and respiratory tract tissues. Serum samples were collected before primary immunization and after booster with PspA-nanogel, PspA alone, or PBS only. The respiratory tract tissues, which included nasal epithelial and lung samples, were collected after booster immunization with PspA-nanogel, PspA alone, or PBS only. Total RNAs were isolated from serum by using TRIzol LS reagent, and from nasal tissue or lung by using TRIzol reagent (Invitrogen) following the manufacturer's protocol. All the miRNAs in the sample were polyadenylated by using poly(A) polymerase and ATP (Invitrogen). Following polyadenylation, SuperScript III RT and a specially designed Universal RT Primer (Invitrogen) were used to synthesize cDNA from the tailed miRNA population. Each of the first-strand cDNAs was analyzed by quantitative RT-PCR with Fast SYBR Green Master Mix and Step One Plus Real-Time PCR System (Applied Biosystems, Carlsbad, CA). The expression levels were normalized to miR-16, which is a commonly used internal control for miRNA expression.[49,50]

Analysis of Ets-1 expression. After total RNAs were isolated from lung tissue, cDNA was synthesized by using PrimeScript RT Master Mix (Takara, Shiga, Japan) following the manufacturer's protocol. The cDNA was analyzed by quantitative RT–PCR with Fast SYBR Green Master Mix and Step One Plus Real-Time PCR System (Applied Biosystems). The PCR primers were used as follows: Ets-1: F, 5′-TGG AGTCAACCCAGCCTATC-3′ and R, 5′-TCTGCAAGGTGTCTGTC TGG-3′; β-actin: F, 5′-TGACGTGGACATCCGCAAAG-3′ and R, 5′-CTGGAAGGTGGACAGCGAGG-3′. The expression levels were normalized to that of β-actin.

Statistical analysis. The results are presented as means ± s.d. Student's *t*-test was used for comparisons among groups. The *P* values <0.05 or <0.01 were considered to indicate statistical significance.

SUPPLEMENTARY MATERIAL is linked to the online version of the paper at http://www.nature.com/mi

ACKNOWLEDGMENTS

This work was supported by the Ministry of Health, Labour, and Welfare of Japan (Y. Y.), Global Center of Excellence Program "Center of Education and Research for the Advanced Genome—Based Medicine—For personalized medicine, the control of worldwide infectious diseases—"MEXT" Japan (Y.F. and H.K.), the Ministry of Education, Culture, Sports, Science, and Technology of Japan (Grant-in-Aid for Scientific Research S [23229004], H.K.), and the Core Research for Evolutional Science and Technology Program of the Japan Science and Technology Agency (H.K.). We are grateful to Drs. Natsumi Takeyama, Koji Kashima, and Tatsuhiko Azegami and Mr. Yuji Suzuki for their useful discussions and technical support.

DISCLOSURE

The authors declare no conflict of interest.

REFERENCES

1. Jackson, L.A. & Janoff, E.N. Pneumococcal vaccination of elderly adults: new paradigms for protection. *Clin. Infect. Dis.* **47**, 1328–1338 (2008).
2. Nuorti, J.P. & Whitney, C.G. Prevention of pneumococcal disease among infants and children - use of 13-valent pneumococcal conjugate vaccine and 23-valent pneumococcal polysaccharide vaccine - recommendations of the Advisory Committee on Immunization Practices (ACIP). *MMWR Recomm. Rep.* **59**, 1–18 (2010).
3. Oosterhuis-Kafeja, F., Beutels, P. & Van Damme, P. Immunogenicity, efficacy, safety and effectiveness of pneumococcal conjugate vaccines (1998-2006). *Vaccine* **25**, 2194–2212 (2007).
4. Dagan, R. *et al.* Reduction of nasopharyngeal carriage of Streptococcus pneumoniae after administration of a 9-valent pneumococcal conjugate vaccine to toddlers attending day care centers. *J. Infect. Dis.* **185**, 927–936 (2002).
5. Dagan, R. *et al.* Comparative immunogenicity and efficacy of 13-valent and 7-valent pneumococcal conjugate vaccines in reducing nasopharyngeal colonization: a randomized double-blind trial. *Clin. Infect. Dis.* **57**, 952–962 (2013).
6. Croney, C.M., Coats, M.T., Nahm, M.H., Briles, D.E. & Crain, M.J. PspA family distribution, unlike capsular serotype, remains unaltered following introduction of the heptavalent pneumococcal conjugate vaccine. *Clin. Vaccine Immunol.* **19**, 891–896 (2012).
7. Pilishvili, T. *et al.* Sustained reductions in invasive pneumococcal disease in the era of conjugate vaccine. *J. Infect. Dis.* **201**, 32–41 (2010).

8. Berry, A.M., Yother, J., Briles, D.E., Hansman, D. & Paton, J.C. Reduced virulence of a defined pneumolysin-negative mutant of *Streptococcus pneumoniae*. *Infect. Immun.* **57**, 2037–2042 (1989).
9. McDaniel, L.S. *et al.* Use of insertional inactivation to facilitate studies of biological properties of pneumococcal surface protein A (PspA). *J. Exp. Med.* **165**, 381–394 (1987).
10. Briles, D.E. *et al.* Intranasal immunization of mice with a mixture of the pneumococcal proteins PsaA and PspA is highly protective against nasopharyngeal carriage of *Streptococcus pneumoniae*. *Infect. Immun.* **68**, 796–800 (2000).
11. Nguyen, C.T., Kim, S.Y., Kim, M.S., Lee, S.E. & Rhee, J.H. Intranasal immunization with recombinant PspA fused with a flagellin enhances cross-protective immunity against *Streptococcus pneumoniae* infection in mice. *Vaccine* **29**, 5731–5739 (2011).
12. McCool, T.L., Cate, T.R., Moy, G. & Weiser, J.N. The immune response to pneumococcal proteins during experimental human carriage. *J. Exp. Med.* **195**, 359–365 (2002).
13. Kono, M., Hotomi, M., Hollingshead, S.K., Briles, D.E. & Yamanaka, N. Maternal immunization with pneumococcal surface protein A protects against pneumococcal infections among derived offspring. *PLoS One* **6**, e27102 (2011).
14. Fukuyama, Y. *et al.* A combination of Flt3 ligand cDNA and CpG oligodeoxynucleotide as nasal adjuvant elicits protective secretory-IgA immunity to *Streptococcus pneumoniae* in aged mice. *J. Immunol.* **186**, 2454–2461 (2011).
15. Ferreira, D.M. *et al.* Characterization of protective mucosal and systemic immune responses elicited by pneumococcal surface protein PspA and PspC nasal vaccines against a respiratory pneumococcal challenge in mice. *Clin. Vaccine Immunol.* **16**, 636–645 (2009).
16. Fukuyama, Y. *et al.* Secretory-IgA antibodies play an important role in the immunity to *Streptococcus pneumoniae*. *J. Immunol.* **185**, 1755–1762 (2010).
17. Janoff, E.N. *et al.* Killing of *Streptococcus pneumoniae* by capsular polysaccharide-specific polymeric IgA, complement, and phagocytes. *J. Clin. Invest.* **104**, 1139–1147 (1999).
18. Ayame, H., Morimoto, N. & Akiyoshi, K. Self-assembled cationic nanogels for intracellular protein delivery. *Bioconjug. Chem.* **19**, 882–890 (2008).
19. Nochi, T. *et al.* Nanogel antigenic protein-delivery system for adjuvant-free intranasal vaccines. *Nat. Mater.* **9**, 572–578 (2010).
20. Yuki, Y. *et al.* Nanogel-based antigen-delivery system for nasal vaccines. *Biotechnol. Genet. Eng. Rev.* **29**, 61–72 (2013).
21. Kong, I.G. *et al.* Nanogel-based PspA intranasal vaccine prevents invasive disease and nasal colonization by *Streptococcus pneumoniae*. *Infect. Immun.* **81**, 1625–1634 (2013).
22. Baltimore, D., Boldin, M.P., O'Connell, R.M., Rao, D.S. & Taganov, K.D. MicroRNAs: new regulators of immune cell development and function. *Nat. Immunol.* **9**, 839–845 (2008).
23. O'Connell, R.M., Rao, D.S., Chaudhuri, A.A. & Baltimore, D. Physiological and pathological roles for microRNAs in the immune system. *Nat. Rev. Immunol.* **10**, 111–122 (2010).
24. Zhu, S., Pan, W. & Qian, Y. MicroRNA in immunity and autoimmunity. *J. Mol. Med.* **91**, 1039–1050 (2013).
25. Cobb, B.S. *et al.* T cell lineage choice and differentiation in the absence of the RNase III enzyme Dicer. *J. Exp. Med.* **201**, 1367–1373 (2005).
26. Muljo, S.A. *et al.* Aberrant T cell differentiation in the absence of Dicer. *J. Exp. Med.* **202**, 261–269 (2005).
27. Koralov, S.B. *et al.* Dicer ablation affects antibody diversity and cell survival in the B lymphocyte lineage. *Cell* **132**, 860–874 (2008).
28. Kitano, S. *et al.* HER2-specific T-cell immune responses in patients vaccinated with truncated HER2 protein complexed with nanogels of cholesteryl pullulan. *Clin. Cancer Res.* **12**, 7397–7405 (2006).
29. van Ginkel, F.W., Jackson, R.J., Yuki, Y. & McGhee, J.R. Cutting edge: the mucosal adjuvant cholera toxin redirects vaccine proteins into olfactory tissues. *J. Immunol.* **165**, 4778–4782 (2000).
30. Yuki, Y. & Kiyono, H. Mucosal vaccines: novel advances in technology and delivery. *Expert Rev. Vaccines* **8**, 1083–1097 (2009).
31. Illum, L. Is nose-to-brain transport of drugs in man a reality? *J. Pharm. Pharmacol.* **56**, 3–17 (2004).
32. Yuki, Y. *et al.* In vivo molecular imaging analysis of a nasal vaccine that induces protective immunity against botulism in nonhuman primates. *J. Immunol.* **185**, 5436–5443 (2010).
33. Fukuyama, Y. *et al.* Novel vaccine development strategies for inducing mucosal immunity. *Expert Rev. Vaccines* **11**, 367–379 (2012).
34. Twigg, H.L. 3rd Humoral immune defense (antibodies): recent advances. *Proc. Am. Thorac. Soc.* **2**, 417–421 (2005).
35. Baumjohann, D. & Ansel, K.M. MicroRNA-mediated regulation of T helper cell differentiation and plasticity. *Nat. Rev. Immunol.* **13**, 666–678 (2013).
36. Li, Q.J. *et al.* miR-181a is an intrinsic modulator of T cell sensitivity and selection. *Cell* **129**, 147–161 (2007).
37. Vigorito, E. *et al.* microRNA-155 regulates the generation of immunoglobulin class-switched plasma cells. *Immunity* **27**, 847–859 (2007).
38. Chen, C.Z., Li, L., Lodish, H.F. & Bartel, D.P. MicroRNAs modulate hematopoietic lineage differentiation. *Science* **303**, 83–86 (2004).
39. Tan, L.P. *et al.* miRNA profiling of B-cell subsets: specific miRNA profile for germinal center B cells with variation between centroblasts and centrocytes. *Lab. Invest.* **89**, 708–716 (2009).
40. Ventura, A. *et al.* Targeted deletion reveals essential and overlapping functions of the miR-17 through 92 family of miRNA clusters. *Cell* **132**, 875–886 (2008).
41. Kang, S.G. *et al.* MicroRNAs of the miR-17-92 family are critical regulators of T(FH) differentiation. *Nat. Immunol.* **14**, 849–857 (2013).
42. Lu, Y.J. *et al.* Interleukin-17A mediates acquired immunity to pneumococcal colonization. *PLoS Pathog.* **4**, e1000159 (2008).
43. Malley, R. *et al.* $CD4^+$ T cells mediate antibody-independent acquired immunity to pneumococcal colonization. *Proc. Natl. Acad. Sci. USA* **102**, 4848–4853 (2005).
44. Trzcinski, K. *et al.* Protection against nasopharyngeal colonization by *Streptococcus pneumoniae* is mediated by antigen-specific $CD4^+$ T cells. *Infect. Immun.* **76**, 2678–2684 (2008).
45. Jaffar, Z., Ferrini, M.E., Herritt, L.A. & Roberts, K. Cutting edge: lung mucosal Th17-mediated responses induce polymeric Ig receptor expression by the airway epithelium and elevate secretory IgA levels. *J. Immunol.* **182**, 4507–4511 (2009).
46. Hirota, K. *et al.* Plasticity of Th17 cells in Peyer's patches is responsible for the induction of T cell-dependent IgA responses. *Nat. Immunol.* **14**, 372–379 (2013).
47. Wright, A.K. *et al.* Experimental human pneumococcal carriage augments IL-17A-dependent T-cell defence of the lung. *PLoS Pathog.* **9**, e1003274 (2013).
48. Du, C. *et al.* MicroRNA miR-326 regulates TH-17 differentiation and is associated with the pathogenesis of multiple sclerosis. *Nat. Immunol.* **10**, 1252–1259 (2009).
49. Chang, K.H., Mestdagh, P., Vandesompele, J., Kerin, M.J. & Miller, N. MicroRNA expression profiling to identify and validate reference genes for relative quantification in colorectal cancer. *BMC Cancer* **10**, 173 (2010).
50. Mizuno, H. *et al.* Identification of muscle-specific microRNAs in serum of muscular dystrophy animal models: promising novel blood-based markers for muscular dystrophy. *PLoS One* **6**, e18388 (2011).

Gene Therapy (2014), 1–10

www.nature.com/gt

ORIGINAL ARTICLE

Vero/BC-F: an efficient packaging cell line stably expressing F protein to generate single round-infectious human parainfluenza virus type 2 vector

J Ohtsuka[1,2], M Fukumura[1,2], M Tsurudome[1], K Hara[1], M Nishio[1,3], M Kawano[1] and T Nosaka[1]

A stable packaging cell line (Vero/BC-F) constitutively expressing fusion (F) protein of the human parainfluenza virus type 2 (hPIV2) was established for production of the *F*-defective and single round-infectious hPIV2 vector in a strategy for recombinant vaccine development. The *F* gene expression has not evoked cytostatic or cytotoxic effects on the Vero/BC-F cells and the F protein was physiologically active to induce syncytial formation with giant polykaryocytes when transfected with a plasmid expressing hPIV2 hemagglutinin-neuraminidase (*HN*). Transduction of the *F*-defective replicon RNA into the Vero/BC-F cells led to the release of the infectious particles that packaged the replicon RNA (named as hPIV2ΔF) without detectable mutations, limiting the infectivity to a single round. The maximal titer of the hPIV2ΔF was 6.0×10^8 median tissue culture infections dose per ml. The influenza A virus *M2* gene was inserted into hPIV2ΔF, and the M2 protein was found to be highly expressed in a human lung cancer cell line after transduction. Furthermore, *in vivo* airway infection experiments revealed that the hPIV2ΔF was capable of delivering transgenes to hamster tracheal cells. Thus, non-transmissible or single round-infectious hPIV2 vector will be potentially applicable to human gene therapy or recombinant vaccine development.

Gene Therapy advance online publication, 19 June 2014; doi:10.1038/gt.2014.55

INTRODUCTION

Human parainfluenza virus type 2 (hPIV2), a member of the *Paramyxovirdae*, has a non-segmented negative-strand RNA genome of approximately 15 kb in length, encoding seven structural proteins, NP, P/V, M, F, HN and L in this order.[1,2] hPIV2 is a respiratory pathogen that causes croup and other upper and lower respiratory tract diseases in young children at the incidence peak between 1 and 2 years of age,[1,3] and a majority of children have been infected with hPIV2 by 5 years of age.[1] hPIVs commonly reinfect children and adults; however, the illness in healthy children and adults is usually limited to the upper respiratory tract.[1]

hPIV2 has two surface glycoproteins, the hemagglutinin-neuraminidase (HN) and fusion (F) protein. hPIV2 attaches to the cell surface receptors via the HN protein, and F protein triggers the envelope-cell fusion. F protein-mediated fusion allows the viral nucleocapsid to enter a host cell. F protein also induces membrane fusion between host cells (syncytial formation).[3] Syncytial formation is one of the characteristics of many enveloped viruses including the paramyxovirus, and has been reported as a potentially important mechanism for virus-induced cytotoxic effects.[3] F protein of the human parainfluenza virus is generated as an inactive precursor (F0) and must be cleaved by endopeptidase to yield an active F protein, which is composed of two disulfide-linked molecules (F1 and F2) and is thought to be required for syncytial formation. The proteolytic cleavage of F protein varies among the different human parainfluenza virus types. In hPIV2 (Toshiba strain)[4] F0 is cleaved into F1 and F2 without the addition of trypsin in the culture medium.[4]

The viral vectors derived from non-segmented negative-stranded RNA viruses such as hPIV2 are supposed to be superior to other transient expression systems because of their high transduction efficiency.[5] In comparison with other viruses, the use of such RNA viruses as a vector is safer because they do not have a DNA phase throughout their life cycles and they replicate exclusively in the cytoplasm, thus avoiding unintended genetic modifications of host cell DNA. These characteristics make the negative-stranded RNA viruses useful as potential vectors for transient high expression.

A method to recover the infectious virus from cloned DNA was established in non-segmented negative-stranded RNA virus (reverse genetics method). The first success was in a rabies virus in which a plasmid DNA encoding a full length of antigenomic viral RNA was used.[6] The development of reverse genetics has made it possible to explore the utility of negative-stranded RNA viruses to deliver foreign genes and has opened the way to gene transfer vectors for therapeutic purposes or vaccine development.[7–10] However, the wild-type hPIV2 vector harbors all the viral structural genes to produce multiple round-infectious hPIV2 replicon particles. Therefore, non-transmissible or a single round-infectious replicon form of the hPIV2 vector is desirable for clinical safety as biopharmaceuticals. It is considered that lack of either an *F* or *HN* envelope gene not only abolishes the progeny generation but also prevents deleterious fusion events to neighboring cells, thus conferring a safety property. Although having a high expression of *F* gene of the parainfluenza virus 5 was reported to be toxic to the infected cells,[11] establishment of

[1]Department of Microbiology and Molecular Genetics, Mie University Graduate School of Medicine, Tsu, Japan and [2]Biocomo Inc., Komono, Komono-cho, Mie, Japan. Correspondence: M Fukumura, Biocomo, Inc. 1325, Komono, Komono-cho, Mie 510-1233, Japan. or Professor T Nosaka, Department of Microbiology and Molecular Genetics, Mie University Graduate School of Medicine, 2-174, Edobashi, Tsu, Mie 514-8507, Japan.
E-mail: m-fukumura@biocomo.jp or nosaka@doc.medic.mie-u.ac.jp
[3]Current Address: Department of Microbiology, Wakayama Medical University, Kimiidera, Wakayama, Japan.
Received 28 August 2013; revised 8 May 2014; accepted 12 May 2014

a stable packaging cell line expressing *F* gene is attractive for the simple and efficient manufacturing process of non-transmissible hPIV2 replicons.

Vero cell line was established from a normal kidney of an adult African green monkey (Cercopithecus) in 1962 by Y Yasumura and Y Kawakita at the Chiba University in Japan.[12] Vero cells do not produce interferons,[13] and are susceptible to infection and proliferation of SV-40, measles virus, arbovirus, reovirus, rubella virus, simian adenovirus, poliovirus, influenza virus, parainfluenza virus, respiratory syncytial virus, vaccinia virus and other viruses.[14] A well-characterized Vero cell line has been used for the production of a number of vaccines against human diseases caused by viruses, including poliomyelitis,[15,16] rabies[16] and others. Therefore, we used the Vero cells to stably express the *F* gene of hPIV2.

Transduction of the replicon RNA lacking an *F* gene (hPIV2ΔF) into the stable Vero packaging cell line expressing F protein led to the release of single round-infectious particles that packaged the replicon RNA with high production efficiency. Here we show that the exogenous gene is expressed efficiently in human lung cancer cells *in vitro* and hamster respiratory tract cells *in vivo* via this novel production system of the recombinant hPIV2ΔF vector.

RESULTS

Stable cell line expressing F protein of hPIV2

To generate a stable Vero cell line constitutively expressing F protein of hPIV2, a pCXN2,[17] which consisted of cytomegalovirus immediate-early enhancer, chicken β-actin promoter and *Neomycin*-resistance gene, was used to construct pCXN2-hPIV2F (Figure 1a), and the expression vector was transfected into Vero cells. Twenty of the G418-resistant clones were isolated 2 to 4 weeks after transfection to evaluate mRNA for the F protein by one-step reverse transcription (RT)-PCR. Consequently, 8 out of 20 G418-resistant clones were selected as F-stable clone candidates, based on the *F* gene expression. Afterwards, the clone with best growth and the highest virion productivity out of the eight F-stable clone candidates was selected and further subjected to limiting dilution. The resultant cells derived from a single cell were designated as Vero/BC-F. The RT-PCR analysis indicated that the amount of *F* gene mRNA in Vero/BC-F cells was nearly equal to that in Vero cells infected with wild-type hPIV2 at a multiplicity of infection (MOI) of 0.2 for 24 h (Figure 1b).

We next investigated syncytial formation with the HN protein of hPIV2. The F protein was not reported to induce cell-to-cell fusion by itself, but to induce when coexpressed with the HN protein.[3] Indeed, transient expression of the *F* gene in control Vero cells induced syncytial formation only with coexpression of the *HN* gene (Figure 1c, bottom panels), disclosing that the F and HN proteins produced after transfection are physiologically active in inducing syncytial formation in Vero cells. Therefore, Vero/BC-F cells were transfected with pSRα-HN.[18,19] The transfected cells similarly made syncytia (giant polykaryocytes) (Figure 1c (upper panels) and d). These results indicate that Vero/BC-F cells produce physiologically active F protein.

Characteristics of the Vero/BC-F cells

As shown in Figure 2a, the Vero/BC-F cells grew almost equally to control Vero cells in the growth medium, indicating that F protein expression did not affect the cell growth in these cells.

The flow cytometry analysis revealed the expression of F protein on the surface of Vero/BC-F cells with an anti-F (144-1A) monoclonal antibody (mAb)[20] (Figure 2b). The amount of F protein in Vero/BC-F cells (red line) was nearly equal to that in Vero cells infected with wild-type hPIV2 at an MOI of 0.2 for 24 h (green line).

Good growth of Vero/BC-F cells was supposed to be attributed to the proper level of F protein expression. To test this, we investigated the effects of overexpression of F protein in Vero/BC-F cells. The cells were transfected with pSRα (pcDL-SRα296)[18] or pSRα-F,[19] and dying cells were stained with propidium iodide (PI). The cells transfected with pSRα-F showed significantly increased numbers of rounding cells and PI-positive cells (Figure 2c), indicating that overexpression of F protein elicited considerable cytotoxicity in Vero/BC-F cells. Furthermore, flow cytometry analysis corroborated the cytotoxicity of the overexpression of F protein (Figure 2d). Therefore, Vero cells could have a threshold within which they are tolerable to the cytotoxicity of F protein.

Subsequently, we examined whether the Vero/BC-F cells could continue to proliferate normally and maintain expressing physiologically active F protein for a long period, using the cells passaged continuously for at least 2.5 years. The cells could continue to grow normally. However, the amount of the *F* gene mRNA in the cells cultured for 2.5 years was decreased to approximately one-fifth of that in the fresh Vero/BC-F cells, by the RT-quantitive PCR (qPCR) analysis (Figure 2e). Accordingly, the efficiency of viral recovery from the long-term passaged Vero/BC-F cells was reduced to about one-sixth at day 3 and a half at day 6 after infection of EGFP-hPIV2ΔF at an MOI of 0.1, compared with that from the fresh cells (Figure 2f).

Recovery of the *F*-defective hPIV2 replicon particles with intact genomic structure

F-defective hPIV2 was constructed from pPIV2[21] with modifications, which harbors an hPIV2 genome of 15 654 nucleotides in length after resequencing. The *F*-defective hPIV2 cDNA with *EGFP* gene as a marker was constructed in accordance with the rule of six (Figure 3a).[22,23] Vero/BC-F cells were transfected with the *F*-defective *EGFP*-hPIV2 cDNA driven by T7 RNA polymerase promoter together with the plasmids that express NP, P and L proteins (polymerase units), and T7 RNA polymerase, respectively, in 6-well plates. After 1 week, half of the culture supernatant was transferred to the culture medium of the fresh Vero/BC-F cells. After incubation for 3 days, some GFP-expressing cells were observed, indicating successful recovery of the *F*-defective hPIV2 replicon particles. The culture supernatant was collected and passed through the 0.45 μm filter to remove cells and cell debris, and then transferred to the fresh Vero/BC-F cells. After a few days, GFP fluorescence spread over the entire cell culture and the infectious particles were collected from the culture supernatant.

Subsequently, we examined whether the infectious particles contained the *F*-defective hPIV2 genome. One-step RT-PCR was carried out with the primers shown in Table 1. The primers were designed to span the entire *F* gene to amplify a 2.2 kbp fragment for the wild-type hPIV2 genome or a 0.37 kbp fragment for the *F*-defective hPIV2 genome. Also, the primers were designed to cover the *M* and *F* gene array to amplify a 0.36 kbp fragment for the wild-type hPIV2 genome or no fragment for the *F*-defective hPIV2 genome. The products of a 2.2 and a 0.36 kbp, and those of a 0.37 kbp and no amplification were observed on the wild-type hPIV2 genome and the *F*-defective hPIV2 genome, respectively (Figure 3b). Moreover, the amplified fragment within the *L* gene and that covering the *NP* and *P* genes confirmed that the particles have the genome of hPIV2 lacking the *F* gene (Figure 3b). In addition, the direct sequencing of the whole viral genome of the particles revealed that the entire *F* gene was deleted in the genome of the particles and the rest of the hPIV2 genome was correctly maintained even after 4, 7 and 10 rounds of viral passage in triplicate (data not shown). It was thus proven that the infectious particles have the genome of hPIV2 devoid of the whole *F* gene. The infectious particles were designated as EGFP-hPIV2ΔF.

Next, the expression of the HN or F protein was investigated in control Vero cells infected with the wild-type hPIV2 or the

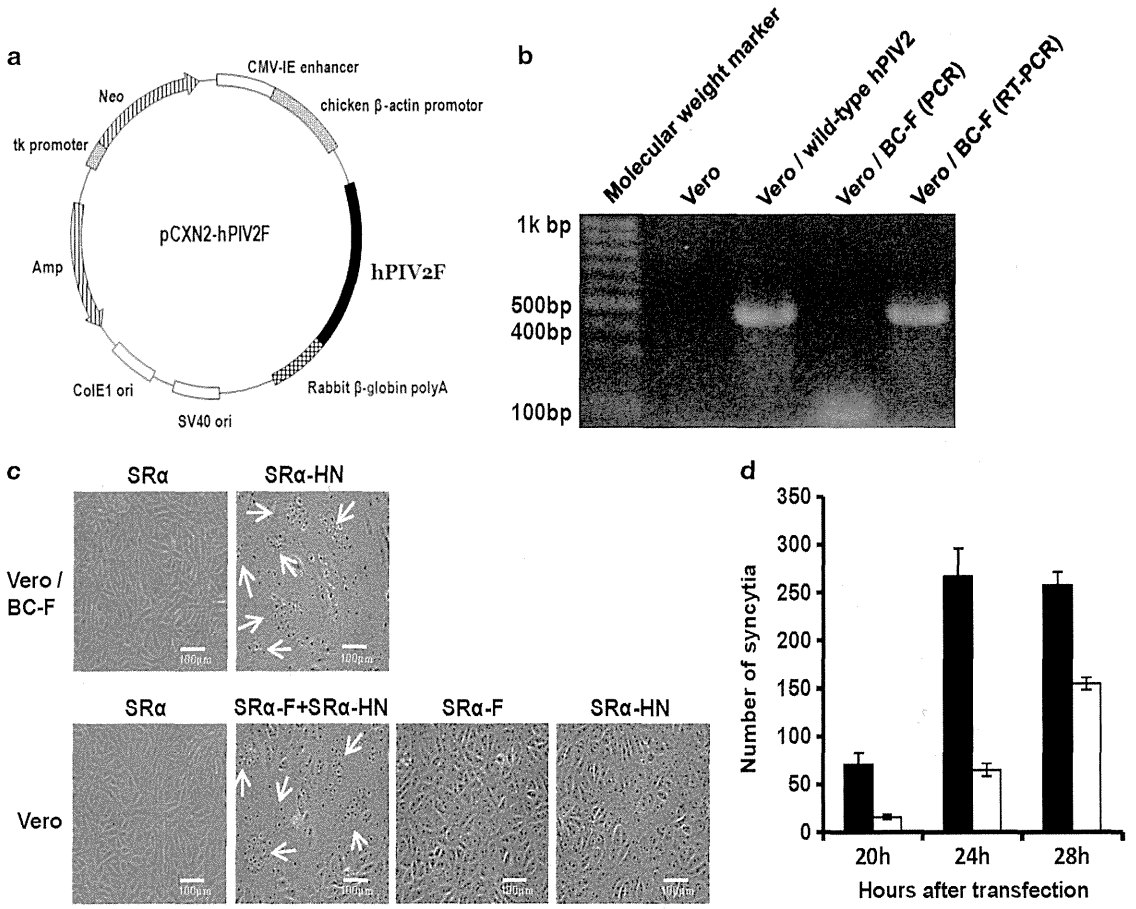

Figure 1. Generation and characterization of the stable Vero cell line constitutively expressing hPIV2 F protein. (**a**) Schematic representation of the recombinant plasmid used in this experiment. A coding sequence of the F protein of hPIV2 was amplified by PCR and inserted into pCXN2. (**b**) Ascertainment of mRNA encoding the F protein in Vero/BC-F cells by one-step RT-PCR. A sample without RT was used as a negative control (labeled as (PCR)). (**c**) Cell fusion induced by coexpression of hPIV2 HN protein in Vero/BC-F cells. Control Vero cells were also transfected with pSRα-F and/or pSRα-HN, or pSRα. Arrows indicate syncytia. (**d**) Quantification of the syncytia formation induced by coexpression of hPIV2 F and HN proteins. Numbers of syncytia in Vero/BC-F cells transfected with pSRα-HN (black columns) and control Vero transfected with pSRα-F and pSRα-HN (white columns) were counted 20, 24 and 28 h after transfection. All the data are shown as mean ± s.d.

EGFP-hPIV2ΔF at an MOI of 5 by cell surface biotinylation and immunoprecipitation methods.[24,25] The viral glycoproteins were immunoprecipitated from the cell lysate with either an anti-HN (108-S1)[20] or the anti-F (144-1A) mAb. As shown in Figure 3c, the EGFP-hPIV2ΔF gave no detectable bands with the anti-F mAb at 24 and 72 h postinfection, but a weak band with the anti-HN mAb at 24 h, followed by a dense band at 72 h postinfection. In contrast, wild-type hPIV2 showed dense bands both with the anti-HN and anti-F mAbs at 24 h postinfection. These results indicate that because of the *F* gene deficiency, the hPIV2ΔF could not express the F protein from the genome, and required the F protein expressed *in trans* for infectious virus production. Moreover, it was considered that the assembly of the EGFP-hPIV2ΔF could be delayed relative to that of the wild-type hPIV2 at 24 h after infection (Figure 3c), as the expression level of the HN protein of the EGFP-hPIV2ΔF was significantly lower than that of the wild-type hPIV2 at 24 h after infection at an MOI of 5.

To examine whether the EGFP-hPIV2ΔF RNA could be encapsidated in single round-infectious particles in an F protein-dependent manner, the spread of GFP-positive cells was investigated in the Vero/BC-F cells and control Vero cells, which were infected with the EGFP-hPIV2ΔF at an MOI of 0.1. Two days after the infection, there was a small difference in the number of GFP-positive cells between both cells. Four and six days later, however, strong fluorescence significantly spread over the entire area in the Vero/BC-F cells, whereas it did not in the control Vero cells (Figure 3d). Furthermore, flow cytometry analysis disclosed markedly increased expression of GFP in Vero/BC-F cells, but not in Vero cells (Figure 3e). Therefore, the increase of GFP-positive cells depended on the F protein expression, indicating that the EGFP-hPIV2ΔF particles are non-transmissible replicon particles after single round infection.

Subsequently, the growth of the EGFP-hPIV2ΔF and wild-type hPIV2 was assessed. The EGFP-hPIV2ΔF showed no propagation when cultured in control Vero cells. On the other hand, the EGFP-hPIV2ΔF in Vero/BC-F cells and wild-type hPIV2 cultured in the control Vero cells propagated vigorously 2–4 days after infection to generate a maximal infectious titer of 6.0×10^8 and 9.0×10^8 median tissue culture infective dose ($TCID_{50}$) per ml, respectively (Figure 3f). The viral titer of wild-type hPIV2 cultured in Vero/BC-F cells increased approximately 10-fold, compared with that in the parental Vero cells 3 days after infection, but that in Vero cells finally reached almost equal to that in Vero/BC-F cells by the sixth day after infection (data not shown).

Although homologous recombination has not been reported in the genome of non-segmented negative-stranded RNA viruses,[26] the appearance of a recombinated hPIV2 genome was examined by GFP expression as an indicator. The number of GFP-positive cells did not increase in the control Vero cells infected at an MOI of 0.1 with the EGFP-hPIV2ΔF, which were passaged on the Vero/BC-F

cells more than 10 times, whereas it increased in the Vero/BC-F cells (data not shown). Moreover, no extra bands suggesting acquisition of the *F* gene-containing fragments were detected by the one-step RT-PCR analysis with the primers iii shown in Figure 3a and Table 1 in the culture supernatant containing EGFP-hPIV2ΔF, which were passaged on Vero/BC-F cells more than 10 times. The same results were obtained by three independent experiments. Taken together, it was ascertained that the hPIV2ΔF is not likely to generate replication-competent hPIV2 by homologous recombination in the Vero/BC-F cells.

Expression of influenza M2 protein by M2-hPIV2ΔF in human cells

In an attempt to develop a potential universal influenza vaccine, we constructed a phPIV2ΔF harboring M2 gene of the influenza A

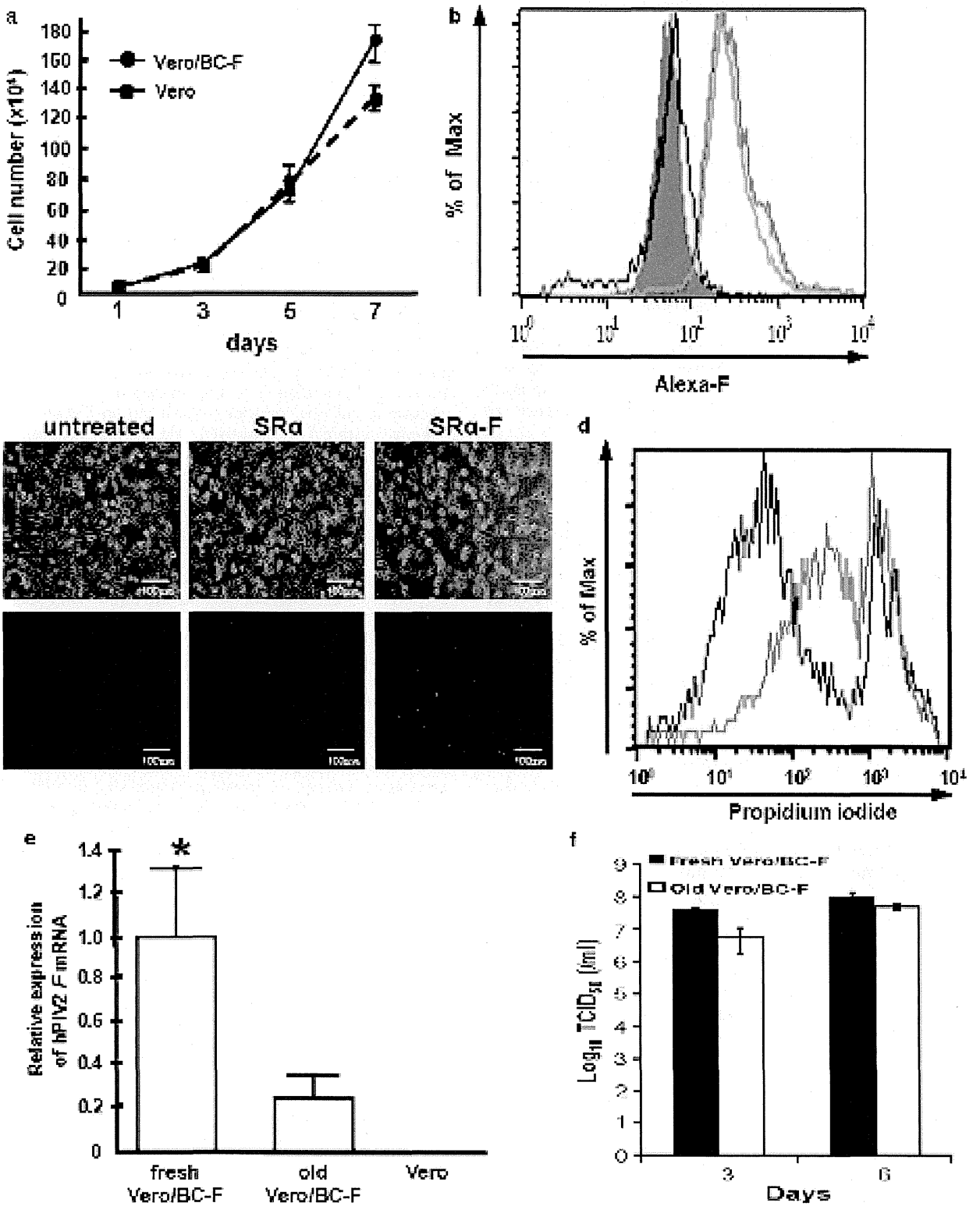

virus (referred to as pM2-hPIV2ΔF). The M2-hPIV2ΔF viruses were successfully recovered by the reverse genetics method using pM2-hPIV2ΔF. To examine M2 protein expression from the M2-hPIV2ΔF, human lung cancer cell line A549 cells were infected with either the M2-hPIV2ΔF or the EGFP-hPIV2ΔF at an MOI of 5 for 2 days. A western blot analysis revealed the M2 protein expression only in M2-hPIV2ΔF-infected cells with strong intensity, whereas hPIV2 NP protein was detected both in M2-hPIV2ΔF- and EGFP-hPIV2ΔF-infected cells (Figure 4). The M2-hPIV2ΔF viruses were recovered in nearly the same high titer as in the EGFP-hPIV2ΔF viruses by using Vero/BC-F cells (data not shown).

Transgene expression in the respiratory tract of the hamsters infected with EGFP-hPIV2ΔF

To investigate the infectivity of the hPIV2ΔF vector and property of the transgene expression *in vivo*, 4-week-old female Syrian hamsters were inoculated intranasally with 7.5×10^8 cell infectious units of the EGFP-hPIV2ΔF. Three days after infection, the tracheas and lungs were harvested and GFP expression was observed under fluorescence microscopy to evaluate the transduction efficiency. Tracheal cells of the EGFP-hPIV2ΔF-administered hamsters showed prominent GFP expression, but none were observed in PBS-administered hamsters (Figures 5a and b). The speckled pattern of the GFP expression in the tracheas is noteworthy because it suggests that the cell-to-cell spread seldom takes place *in vivo* in this system. GFP expression in the lungs was below the detection level (data not shown). These results indicate that the hPIV2ΔF vector is suitable to deliver and express an exogenous gene through the respiratory tract.

DISCUSSION

The application of RNA viral vectors for gene delivery has been hampered owing to difficulty in establishing stable packaging cell lines to generate sufficient amounts of single round-infectious viral vectors of high quality in the manufacturing process. Among human parainfluenza viruses, hPIV3 has been used as a vector for vaccine development, based on a replication-competent system,[7] or on a live-attenuated chimeric virus.[27] Live-attenuated vectors such as the vesicular stomatitis virus have been used extensively as an experimental vaccine, and these vectors easily grow to high titers and stimulate potent cellular and humoral immunity.[28–32] However, obtaining regulatory approval of multiround infectious or replication-competent viral vectors is not easy because of concerns regarding potential pathogenicity. Therefore, RNA viral vectors for gene therapy or recombinant vaccines are expected to be engineered into single round-infectious virions to evade dissemination.

We have successfully generated a cell line (Vero/BC-F) that constitutively expresses the hPIV2 F protein to avoid a transient transfection step and a complex inducible gene expression system during the production of the viral vector.

The Vero/BC-F cells derived from a single cell by limiting dilution have been successfully adapted to culture with a serum-free medium, and a master cell bank of the clone has been established, based on the ICH Guideline (data not shown). We could obtain the EGFP-hPIV2ΔF by the reverse genetics method by using the Vero/BC-F cells in high yields. These results would be applicable to manufacture the recombinant vaccines on the regulation. Furthermore, EGFP-hPIV2ΔF vectors were capable of delivering transgenes to tracheal cells in hamsters.

Single round-infectious cytoplasmic RNA vector expressing the foreign gene is a desirable tool to use as a vector for recombinant vaccine development, because of its high efficiency of transduction, safety property and its effect of inducing dendritic cell maturation (adjuvant effect of the vector itself).[5] As a foreign gene, we tried to express the M2 protein of the influenza A virus. M2 protein consists of 97 amino acids, works as a viral ion channel with a proton transport function and has been proposed as one of the candidates for the universal influenza vaccine.[33–35] As shown in this study, hPIV2ΔF could efficiently express M2 protein in human lung cancer cells. This result as well as previous reports[36–38] suggests that a respiratory viral vector-mediated delivery of the antigen is one of the good strategies for vaccine development against various respiratory diseases.

As for the other paramyxoviral vectors carrying a defective genome, the Sendai virus vector that was devoid of an *F* gene was previously generated in a trypsin-dependent manner with the packaging cell line inducibly expressing an F protein by using a Cre-*loxP* system.[39] In contrast to this Sendai virus vector system, our hPIV2ΔF system uses the stably expressed F protein, and cleavage of F protein is trypsin-independent, thus being easy to handle.

One would consider the pre-existing immunity to hPIV2 in humans is an obstacle for the utility of the vector for recombinant vaccines. Although antibodies in serum and cellular immunity have a major role in reducing pathogenic reactions after respiratory tract infection, innate immunity and local mucosal immunity have key roles in the initial phase of protection in each infection. However, most mucosal responses are often short lived. Although a majority of children have been infected with hPIV2 by 5 years of age,[1] hPIV reinfection is known to occur throughout human life,[1,3] because of an incomplete immunity to hPIVs.[3] Interestingly, the hPIV2 genome was reported to be detected in only 1–3% of cases among children with respiratory diseases,[1,40] suggesting rarity of hPIV2 infection itself in comparison with other respiratory viruses, or weak pathogenicity of hPIV2. We have designed that hPIV2ΔF vector has a cloning site for exogenous gene insertion in the most upstream region within the vector genome to guarantee the preferential expression of the transgene compared with other viral backbone genes. Nevertheless, further

Figure 2. Characteristics of the Vero/BC-F cells. (**a**) Growth of the Vero/BC-F cells. Cells (5.0×10^4) were prepared in 6-well plates and cultured in the growth medium. The numbers of the cells were counted on various days. All the data are shown as mean ± s.d. (**b**) Cell surface expression of the F protein in Vero/BC-F cells. The overlay histograms show expression of hPIV2 F proteins on the cell surface. Vero (gray area), Vero/BC-F (green line) and Vero cells infected with wild-type hPIV2 (red line) were incubated with the specific antibody for hPIV2 F protein. Vero cells infected with wild-type hPIV2, treated with control IgG, were shown as a black line. All the cells were labeled with an Alexa Fluor 488-conjugated anti-mouse IgG antibody. (**c**) The effect of the overexpressed F protein on the Vero/BC-F cells. The Vero/BC-F cells were transfected with the plasmid shown above each panel, and incubated at 37 °C for 48 h. Cytotoxicity was evaluated morphologically and by PI staining. (**d**) Flow cytometry analysis on cell damage by overexpression of hPIV2 F protein in the Vero/BC-F cells. The Vero/BC-F cells transfected with pSRα-F or pSRα were incubated for 48 h, and the cells were stained with PI without fixation (red line, pSRα-F; black line, pSRα). (**e**) Comparison of expression levels of hPIV2 F mRNA in short- and long-term cultured Vero/BC-F cells by RT-qPCR. The same amounts of total RNAs from short-term (fresh Vero/BC-F) and long-term (old Vero-BC-F) cultured cells, and from control Vero cells were reverse transcribed, followed by qPCR. Fresh Vero/BC-F cells were cultured within a few months, and old Vero/BC-F cells were cultured for more than 2.5 years. Relative quantities of hPIV2 F transcripts are shown as mean ± s.d., and the statistical significance ($^*P < 0.05$) was determined by the Bonferroni test. (**f**) Comparison of virus recovery from short- and long-term cultured Vero/BC-F cells. The same new and old cells (1×10^6) as in Figure 2e were infected with the EGFP-hPIV2ΔF at an MOI of 0.1, and the supernatant was collected on 3 and 6 days after infection, followed by titration by the $TCID_{50}$ method. All the data are shown as mean ± s.d.

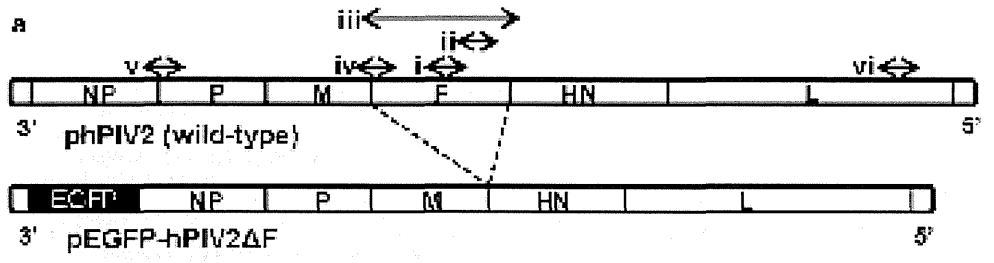

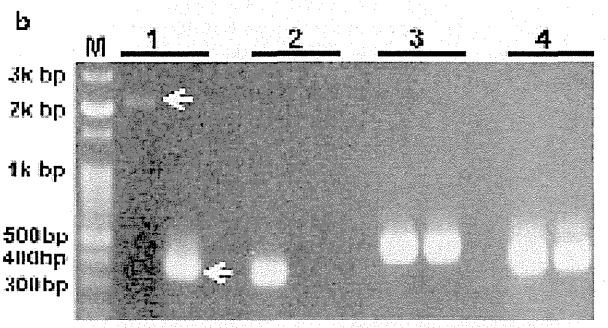

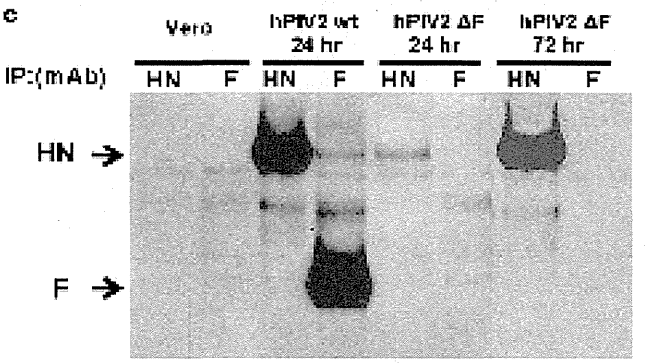

Left column :
wild-type hPIV2/Vero
Right column :
EGFP-hPIV2ΔF/Vero/BC-F
M : Molecular weight marker

Regions amplified
1 between M and HN (Table 1.iii)
2 between M and F (Table 1.iv)
3 between NP and P (Table 1.v)
4 L internal (Table 1.vi)

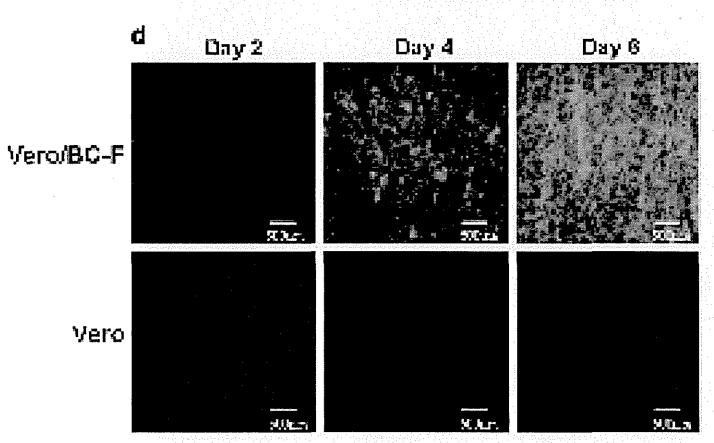

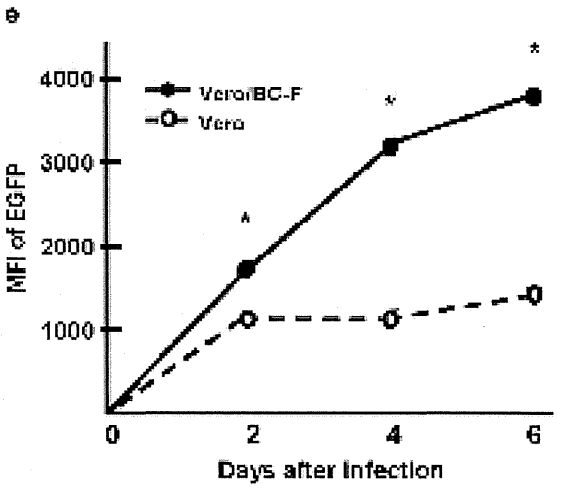

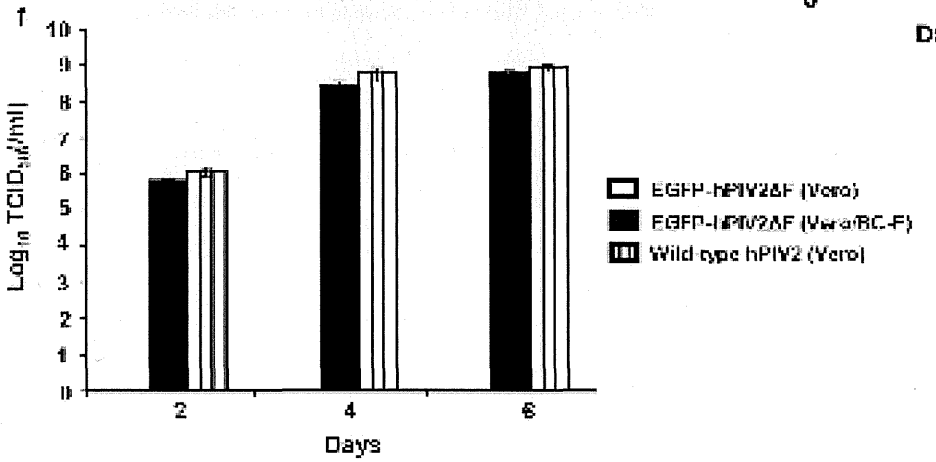

studies are required to see the impact of pre-existing immunity to the vector on the efficiency as a recombinant vaccine.

As for the application of the vector to gene therapy, particularly for the treatment of hereditary diseases due to genetic defects, or cancer therapy, a long-lasting expression of therapeutic genes in high levels in wide varieties of cell types or organs is required. The hPIV2ΔF has an ability to deliver genes efficiently; however, transgene expression will be limited by dilution in actively dividing cells, or might be abrogated by induction of anti-hPIV2 immune responses in addition to pre-existing immunity to hPIV2. Therefore, non- or less-dividing cells would be appropriate targets in gene therapy by the hPIV2ΔF vector. Furthermore, we need to study the therapeutic effects and immune reactions in repeated infection of hPIV2ΔF *in vivo*.

hPIV2ΔF itself may also be used for another purpose. Currently, genome-modified human hPIV2, as a potential vaccine candidate delivered as nose drops, is in phase I of clinical trial for adults, children and infants. The virus has a 3′ genomic promoter mutation and L polymerase mutations that result in virus attenuation.[41] In African green monkeys, immunization with the virus conferred a high level of protection in the upper and lower respiratory tracts of the challenged animals with wild-type hPIV2.[41] Here, we advocate hPIV2ΔF as another potential vaccine candidate against the wild-type hPIV2 because of its property limiting to single round infectivity with no cell-to-cell spread.

In summary, we have generated an *F*-defective hPIV2 vector together with a high-efficiency packaging cell line for recombinant vaccine development.

MATERIALS AND METHODS

Cells, virus and plasmid construction

The Vero cell line was obtained from RIKEN BioResource center (Tsukuba, Japan) and cultured in a minimal essential medium (MEM) (Sigma, St Louis, MO, USA) supplemented with 10% heat-inactivated fetal bovine serum (FBS) (Thermo Fisher Scientific Inc., Waltham, MA, USA). The A549 human lung cancer cell line and MDCK (Madin–Darby canine kidney) cell line were cultured in MEM with 10% FBS. The hPIV2 used was a Toshiba strain.[4] The influenza virus used an A/Puerto Rico/1934 (H1N1) (PR8 strain). The hPIV2 *F* gene was amplified from pPIV2[21] by PCR with tagged primers and cloned into a multicloning site of pCXN2[17] containing a *neomycin-resistance gene* to generate pCXN2-hPIV2F (Figure 1a).

An entire reading frame of the *F* gene was deleted from pPIV2 by using the two-step overlap-primer PCR method to generate *F*-defective hPIV2 cDNA driven by T7 promoter, which was designated as phPIV2ΔF. The *EGFP* gene was amplified by PCR using pEGFP-N1 (Clontech, Palo Alto, CA, USA) as a template and a pair of *NotI*-tagged primers of 5′-ATTGAT TGCGGCCGCGGTCGCCACCATGGTGAGCAAGGGCGAGGAGC-3′ and 5′-ATTG ATTGCGGCCGCCTAACCCGTCCGGGCCTATGATTTTTTCTTAAATTATGAGAGTT ACTTGTACAGCTCGTCCATG-3′ containing hPIV2 *NP* (R2)-intergenic-hPIV2 *P* (R1) sequences, cloned into the *NotI* site just upstream of the *NP* gene of phPIV2ΔF, and was designated as pEGFP-hPIV2ΔF. The influenza A virus *M2* gene tagged with an intervening sequence of hPIV2 was amplified by the one-step RT-PCR (Qiagen, Hilden, Germany) by using 2 μg of purified genomic RNA of PR8, which was obtained from supernatants of MDCK cell cultures after infection at an MOI of 0.1 by using a High Pure Viral RNA Kit (Roche, Indianapolis, IN, USA). The primers used were as follows: 5′-AAAAAGCGGCCGCATAGGTCGCCACCATGAGTCTTCTAACCGAGGTCGAAAC *GCCTATCAGAAACGAATGG*-3′ (a forward primer containing a *NotI* site and fusion sequence of 1–26 (underlined) and 715–733 (italic) of matrix (*M*) gene) and 5′-AAAAAGCGGCCGCCTAACCCGTCCGGGCCTATGATTTTTTCTTA AATTATGAGAGTTATTACTCCAGCTCTATGC-3′ (a reverse primer containing

Table 1. Primer pairs for RT-PCR or RT-qPCR

Target[a]	*Sequences of paired primers (5′–3′)*[b]	*Length of the amplified product (kbp)*
i: F internal (Figure 1b)	CTCAGTTCCGGACTGTTAAC GGGATACAACATGGGGGGGG	0.44
ii: F internal (Figure 2e)	AGCCAAGACACTTTATTCAC TTTCCATGGTTATTCTTGG	0.19
iii: M–HN (Figure 3b)	AGAATAGAACCACAATCAAG GGCAGTTCGGAAAATGATTC	Wt: 2.2 ΔF: 0.37
iv: M–F (Figure 3b)	AGAATAGAACCACAATCAAG CATGTTCCATTGCTTGGGGG	Wt: 0.36 ΔF: no detection
v: NP–P Figure 3b)	GGACAACCAAACAACCAGAC CTGTTCCCAGTCCAGCATGG	Wt and ΔF: 0.48
vi: L internal (Figure 3b)	CTGCATTTCCCAGTAACAAC GAAGCACCGCTTCCTTCGGC	Wt and ΔF: 0.42

Abbreviations: ΔF, hPIV2ΔF; Wt, wild-type hPIV2. [a]Amplified region within hPIV2 genome. [b]Each primer shown in the lower line was also used for RT, except the primer shown in ii where the oligo (dT) primer was used for RT.

Figure 3. Recovery of non-transmissible or single round-infectious hPIV2 replicon particles from the Vero/BC-F cells. (**a**) Construction of hPIV2 cDNA defective in the gene encoding F protein. hPIV2 cDNA lacking the gene encoding the F protein was constructed by removing the entire *F* gene and adding the *EGFP* gene as a marker just upstream of the gene encoding nucleocapsid protein (NP). The PCR products shown in Table 1 are indicated by two-way arrows. (**b**) Certification by RNA analyses for generation of hPIV2 defective in the *F* gene. RNAs from virus particles of wild-type hPIV2/Vero and EGFP-hPIV2ΔF/Vero/BC-F were subjected to one-step RT-PCR using the various primer sets shown in Table 1. (**c**) Expression of F or HN protein on cell surface of Vero cells infected with wild-type hPIV2 or EGFP-hPIV2ΔF. Vero cells were infected with wild-type hPIV2 (hPIV2 wt) or the EGFP-hPIV2ΔF (hPIV2ΔF) at an MOI of 5, and cell surface proteins were biotinylated 24 and 72 (EGFP-hPIV2ΔF only) hours after infection, and were immunoprecipitated with the anti-F and anti-HN mAbs, respectively. The precipitates were subjected to sodium dodecyl sulfate-polyacrylamide gel electrophoresis, followed by nitrocellulose membrane transfer. The biotinylated proteins on the membrane were detected by enhanced chemiluminescence. (**d**) Spread of GFP expression in the Vero/BC-F cells. Confluent monolayers of the control Vero cells and the Vero/BC-F cells in 6-well plates were inoculated with the EGFP-hPIV2ΔF at an MOI of 0.1, and cultured for the time indicated: upper row, Vero/BC-F cells; lower row, control Vero cells. (**e**) Time-dependent increase of EGFP expression in Vero/BC-F cells after infection with hPIV2ΔF. Mean fluorescence intensities (MFIs) of EGFP are shown in Vero/BC-F cells and control Vero cells, both of which were infected with hPIV2ΔF. Data are shown as means ± s.d., and the statistical significance ($^*P < 0.05$) was determined by the Bonferroni test. (**f**) The growth of EGFP-hPIV2ΔF in comparison with that of wild-type hPIV2. Control Vero cells were infected with the EGFP-hPIV2ΔF or wild-type hPIV2, and the Vero/BC-F cells were infected with the EGFP-hPIV2ΔF, at an MOI of 0.1. The supernatant was collected on various days after infection, and the titration was performed by the $TCID_{50}$ method. The growth of EGFP-hPIV2ΔF on control Vero cells, that of EGFP-hPIV2ΔF on Vero/BC-F cells and that of wild-type hPIV2 on control Vero cells are shown in open, closed and hatched columns, respectively. All the data are shown as mean ± s.d.

a *Not*I site and hPIV2 *NP* (R2)-intergenic-hPIV2 *P* (R1) sequence array). A *Not*I fragment of the amplified *M2* gene was inserted into a *Not*I site of phPIV2ΔF, which was designated as pM2-hPIV2ΔF.

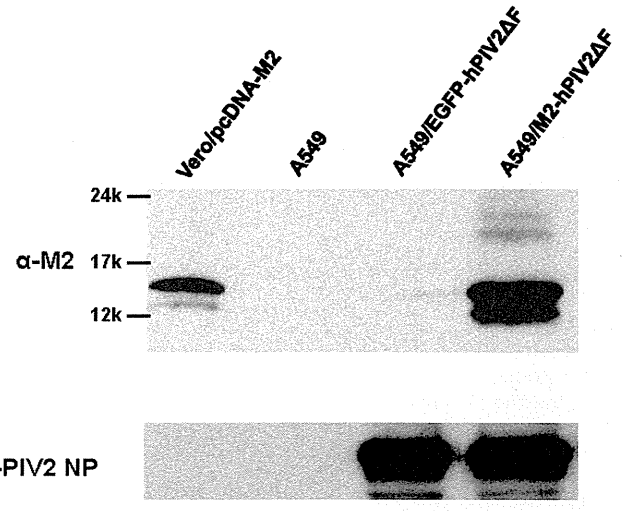

Figure 4. Expression of influenza A virus M2 protein by hPIV2ΔF vector in human lung cancer A549 cells 2 days after infection. The cell lysates were denatured and separated on 5–20% sodium dodecyl sulfate-polyacrylamide gel electrophoresis, and transferred onto a nitrocellulose membrane. The membrane was probed with the mAbs specific to M2 (upper) of the influenza A virus and NP of the hPIV2 (lower), respectively. Vero/pcDNA-M2, Vero cells transfected with pcDNA-M2 as a positive control; A549, non-infected A549 cells as a negative control; A549/EGFP-hPIV2ΔF, A549 cells infected with EGFP-hPIV2ΔF; A549/M2-hPIV2ΔF, A549 cells infected with M2-hPIV2ΔF.

hPIV2 *NP*, *P* and *L* genes were amplified from pPIV2 by PCR and each gene was cloned into pCAGGS.[17] pcDL-SRα296 (pSRα),[18] pSRα-F and pSRα-HN were described previously.[19] The gene encoding T7 RNA polymerase was inserted into an *Eco*RI site of pSRα to generate pSRα-T7 RNA polymerase. An *M2* gene fragment tagged with *Eco*RI and *Xho*I sequences, which was amplified with PCR by using pM2-hPIV2ΔF DNA as a template, was inserted into the corresponding sites of pcDNA to generate pcDNA-M2 for a positive control experiment.

Establishment of the cells constitutively expressing hPIV2 F protein

Vero cells were transfected with 2 μg of pCXN2-hPIV2F DNA with Cell Line Nucleofector Kit V (Lonza, Basel, Switzerland) by using the Amaxa Nucleofector type II (Lonza) according to the manufacturer's instructions and cultured in MEM supplemented with 10% heat-inactivated FBS and 1.0 mg ml^{-1} of G418 (Geneticin) (Thermo Fisher Scientific Inc.) with replacement of the medium two times per week. Cells were cultured for 2–4 weeks and G418-resistant colonies were isolated. To purify single-cell-derived clones, 1×10^4 cells were diluted to 2^{-1} to 2^{-12} with the medium on 96-well plates. A single cell in a well was confirmed by microscopy and was proliferated.

To examine mRNA of the hPIV2 *F* gene, total RNA was extracted with ISOGEN (Nippon Gene, Tokyo, Japan) from 6×10^5 cells of the Vero transfectants with G418 resistance, as well as control Vero cells with and without infection of wild-type hPIV2 at an MOI of 0.2 on the 6-well plates. Total RNA was dissolved in nuclease-free water and each 2 μg of the total RNA was subjected to one-step RT-PCR to amplify the *F* gene using a pair of primers described in Table 1 (i).

For syncytial formation by the F and HN proteins, 1.0×10^6 of the F-stable clone and control Vero cells were cultured in 6-well plates. Control Vero cells were transfected with 1 μg of pSRα-HN and 1 μg of pSRα-F, and Vero cells stably expressing F protein were transfected with 2 μg of pSRα-HN, by using FuGENE HD (Roche) and X-tream GENE HP (Roche). Numbers of syncytia (defined as more than three nuclei aggregation) were counted 20, 24 and 28 h after transfection.

For the cell growth assay, 5.0×10^4 of the control Vero cells and the F-stable clone candidates were initially prepared in 6-well plates and

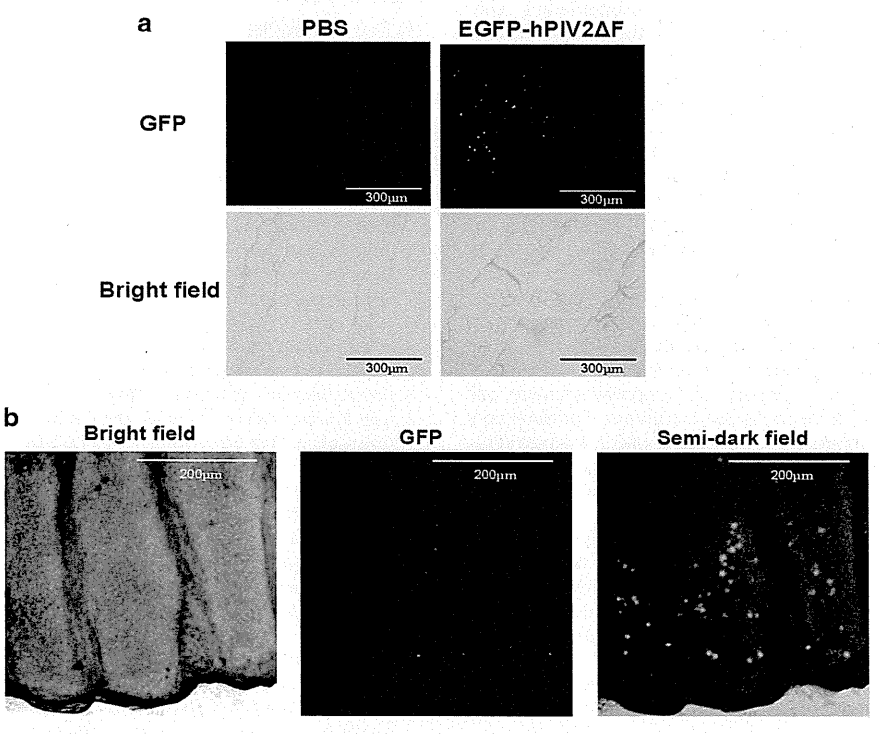

Figure 5. GFP expression in the tracheas of the hamsters after respiratory tract infection of EGFP-hPIV2ΔF. Syrian hamsters were administrated intranasally with EGFP-hPIV2ΔF (7.5×10^8 plaque-forming unit). Three days after infection, GFP expression in the tracheas was observed to evaluate the transduction efficiency. Tracheas were extirpated and the inside of incised tracheas were observed with a fluorescence stereoscopic microscope (Olympus, Tokyo, Japan; SZX7) (**a**) and an inverted fluorescence microscope (Olympus CKX41) (**b**, EGFP-hPIV2ΔF only).

cultured in MEM supplemented with 10% heat-inactivated FBS (growth medium). The cell numbers were counted on various days.

To detect the F protein on the surface, 6×10^5 of control Vero cells, Vero cells infected with wild-type hPIV2 at an MOI of 0.2 and the Vero/BC-F cells were cultured in 6-well plates. Twenty-four hours later, the cells were harvested in a FACS buffer (phosphate-buffered saline (PBS) containing 2% heat-inactivated FBS) and fixed with 4% paraformaldehyde in PBS. Then, the cells were incubated with the anti-F (144-1A) mAb,[20] washed with a FACS buffer three times, labeled with Alexa Flour 488 (Invitrogen, Eugene, OR, USA) and analyzed on a FACSCalibur (BD Biosciences, San Jose, CA, USA) using CellQuest software (BD Biosciences).

To investigate cytotoxicity of overexpressed F protein in the cells, 1.0×10^6 Vero/BC-F cells were transfected with 2 μg of pSRα-F or control pSRα by using X-tream GENE HP. After 2 days, the cells were stained with PI (BioLegend, San Diego, CA, USA) without fixation to evaluate cell damage, and were then analyzed by FACS.

To compare the expression levels of hPIV2 *F* mRNA between the Vero/BC-F cells cultured for a few months and those cultured for more than 2.5 years, an RT-qPCR was carried out. Total RNA was isolated from 1×10^6 cells by using a High Pure RNA Isolation Kit (Roche). The cDNA was synthesized from 1 μg of the total RNA with an oligo $(dT)_{20}$ primer and SuperScript II reverse transcriptase (Invitrogen), according to the manufacturer's instructions. Subsequently, qPCR was performed in triplicate with specific primers shown in Table 1 (ii) for detecting the hPIV2 *F* transcripts. Each reaction contained 10 μl of 2× Power SYBR green master mix (Applied Biosystems/Invitrogen, Foster City, CA, USA), forward and reverse primers and 1 μl of the cDNA products, giving a final reaction volume of 20 μl. qPCR assay was performed on a StepOnePlus real-time PCR system (Applied Biosystems/Invitrogen), and StepOne software v.2.1 (Applied Biosystems/Invitrogen) was used to analyze the qPCR data, according to the manufacturer's instructions. Cycle conditions were set as follows: initial template denaturation at 95 °C for 10 min, followed by 40 cycles of denaturation at 95 °C for 15 s, and annealing/extension at 60 °C for 1 min.

Recovery of a recombinant *F*-defective hPIV2 vector

Vero/BC-F cells were transfected with pEGFP-hPIV2ΔF (10 μg), altogether with each plasmid encoding the hPIV2 *NP* (2 μg), *P* (0.9 μg), *L* (2 μg) and T7 RNA polymerase (3 μg) by using X-tremeGENE HP according to the manufacturer's instructions. One week later, the supernatant was centrifuged to remove cells and cell debris, and was then transferred to the fresh Vero/BC-F cell culture in MEM with 1% heat-inactivated FBS (maintenance medium) for virus propagation.

To examine the recovery of the replicon particles, the Vero/BC-F and Vero cells were infected with the EGFP-hPIV2ΔF viruses produced by reverse genetics and wild-type hPIV2, respectively, at an MOI of 0.1. Seven days later, the supernatant of the transfectants was centrifuged to remove cell debris and viral RNA was isolated with High Pure Viral RNA Kit (Roche). Two μg of purified RNA was subjected to one-step RT-PCR to generate various regions of an hPIV2 genome using the pair of primers shown in Table 1 (iii–vi).

Vero cells (1.0×10^6 cells) were infected with either wild-type hPIV2 or EGFP-hPIV2ΔF at an MOI of 5. The cell surface proteins were biotinylated as described previously.[24,25] The proteins were immunoprecipitated from the cell lysates with the anti-F (144-1A) mAb or the anti-HN (108-S1) mAb.[20] Proteins were separated by sodium dodecyl sulfate-polyacrylamide gel electrophoresis and transferred to nitrocellulose membrane. For detection of biotinylated proteins, the membrane was treated with a streptavidin–biotin–peroxidase complex (Vector Laboratories, Burlingame, CA, USA) and enhanced chemiluminescence reagent, followed by exposure to an X-ray film.

To test the propagation of the EGFP-hPIV2ΔF, 1.0×10^6 cells of the Vero/BC-F or control Vero were inoculated with the EGFP-hPIV2ΔF at an MOI of 0.1. The inoculated cells were incubated in a maintenance medium. The appearance of the GFP fluorescence on the cells was examined 2, 4 and 6 days after inoculation under fluorescence microscopy. Flow cytometry analysis was carried out in the same condition. The Vero/BC-F and Vero cells cultured with EGFP-hPIV2ΔF in various periods were harvested in the FACS buffer, washed two times with the buffer and subjected to FACS analysis.

Also, to test the viral propagation, control Vero cells were infected with the EGFP-hPIV2ΔF or wild-type hPIV2, and the Vero/BC-F cells were infected with the EGFP-hPIV2ΔF at an MOI of 0.1, and incubated in the medium. At appropriate time points, the cultures were examined for production of infectious viruses. The culture supernatant was collected on various days after infection and the virus titer was calculated by the $TCID_{50}$ method. $TCID_{50}$ was determined on 96-well plates as follows: the culture supernatants collected at various time points were diluted to 10^{-4}–10^{-7} with maintenance medium, and each 100 μl was infected to the cells and incubated at 37 °C for 1 week. Virus-positive wells were determined by the presence of cytopathic effects under microscopy.

Expression of M2 protein of the influenza A virus by M2-hPIV2ΔF

A549 cells (1.0×10^6) were infected with the M2-hPIV2ΔF or the EGFP-hPIV2ΔF at an MOI of 5 and incubated with a maintenance medium for 2 days. Cell lysates were subjected to western blot analyses with an anti-M2 (14C2) mAb (Abcam, Cambridge, MA, USA) and an anti-PIV2 NP (20A) mAb,[16] respectively.

Infection of EGFP-hPIV2ΔF to the respiratory tract of hamsters and detection of GFP expression *in vivo*

EGFP-hPIV2ΔF viruses were propagated with Vero/BC-F cells. Cultured supernatants were cleared of the cell debris by centrifugation (2000 *g*, 4 °C, 10 min), followed by ultracentrifugation (141 000 *g*, 4 °C, 30 min) to concentrate the virions. Pellets were dissolved in PBS. Virus titer was determined by $TCID_{50}$. Four-week-old female Syrian hamsters were purchased from Japan SLC (Shizuoka, Japan). Hamsters were anesthetized by intraperitoneal injection of pentobarbital, and EGFP-hPIV2ΔF viruses (7.5×10^8 cell infectious units) in 100 μl of PBS were administered intranasally. Three days after administration, tracheas and lungs were extirpated, and observed under fluorescence microscopy to evaluate the transduction efficiency. All animal studies were approved by the Animal Care Committee of Mie University.

CONFLICT OF INTEREST

JO, MF, MK and TN are patent applicants for Vero/BC-F cells. MF is a founder of Biocomo Inc. MF, MK and TN have shares of stock in Biocomo Inc. JO is an employee of Biocomo Inc.

ACKNOWLEDGEMENTS

We thank Dr Yasuhiro Yasutomi for providing valuable discussions. This work was supported by a Grant-in-Aid for the Regional Innovation R&D Program by the Ministry of Economy, Trade and Industry of Japan.

REFERENCES

1 Karron, RA Collins, PL. Parainfluenza viruses. In: Knipe DM, Howley PM, Cohen JI, Griffin DE, Lamb RA, Martin MA *et al. Fields Virology*, 6th edn. Lippincott Williams & Wilkins: Philadelphia PA, USA, 2013, pp 996–1023.
2 Lamb, RA Parks, GD. Paramyxoviridae. Knipe DM, Howley PM, Cohen JI, Griffin DE, Lamb RA, Martin MA *et al. Fields Virology*, 6th edn. Lippincott Williams & Wilkins: Philadelphia, PA, USA, 2013, pp 957–995.
3 Henrickson KJ. Parainfluenza viruses. *Clin Microbiol Rev* 2003; **16**: 242–264.
4 Ito Y, Tsurudome M, Hishiyama M. The polypeptides of human parainfluenza type 2 virus and their synthesis in infected cells. *Arch Virol* 1987; **95**: 211–224.
5 Hara K, Fukumura M, Ohtsuka J, Kawano M, Nosaka T. Human parainfluenza virus type 2 vector induces dendritic cell maturation without viral RNA replication/transcription. *Hum Gene Ther* 2013; **24**: 683–691.
6 Schnell MJ, Mebatsion T, Conzelmann KK. Infectious rabies viruses from cloned cDNA. *EMBO J* 1994; **13**: 4195–4203.
7 Tang RS, MacPhail M, Schickli JH, Kaur J, Robinson CL, Lawlor HA *et al.* Parainfluenza virus type 3 expressing the native or soluble fusion (F) protein of respiratory syncytial virus (RSV) confers protection from RSV infection in African green monkeys. *J Virol* 2004; **78**: 11198–11207.
8 Tompkins SM, Lin Y, Leser GP, Kramer KA, Haas DL, Howerth EW *et al.* Recombinant parainfluenza virus 5 (PIV5) expressing the influenza A virus hemagglutinin provides immunity in mice to influenza A virus challenge. *Virology* 2007; **362**: 139–150.
9 Zhan X, Slobod KS, Krishnamurthy S, Luque LE, Takimoto T, Jones B *et al.* Sendai virus recombinant vaccine expressing hPIV-3 HN or F elicits protective immunity and combines with a second recombinant to prevent hPIV-1, hPIV-3 and RSV infections. *Vaccine* 2008; **26**: 3480–3488.
10 DiNapoli JM, Yang L, Samal SK, Murphy BR, Collins PL, Bukreyev A. Respiratory tract immunization of non-human primates with a Newcastle disease

virus-vectored vaccine candidate against Ebola virus elicits a neutralizing antibody response. *Vaccine* 2010; **29**: 17–25.
11 Manuse MJ, Parks GD. Role for the paramyxovirus genomic promoter in limiting host cell antiviral responses and cell killing. *J Virol* 2009; **83**: 9057–9067.
12 Yasumura Y, Kawakita Y. Studies on SV40 in tissue culture-preliminary step for cancer research *'in vitro'*. *Nihon Rinsho* 1963; **21**: 1201–1215; in Japanese.
13 Desmyter J, Melnick JL, Rawls WE. Defectiveness of interferon production and of rubella virus interference in a line of African green monkey kidney cells (Vero). *J Virol* 1968; **2**: 955–961.
14 Sheets R. History and characterization of the vero cell line. *The Vaccines and Related Biological Products Advisory Committee Meeting*, Silver spring, MD, USA, 2000.
15 Montagnon BJ, Fanget B, Nicolas AJ. The large-scale cultivation of VERO cells in micro-carrier culture for virus vaccine production. Preliminary results for killed poliovirus vaccine. *Dev Biol Stand* 1981; **47**: 55–64.
16 Montagnon BJ. Polio and rabies vaccines produced in continuous cell lines: a reality for Vero cell line. *Dev Biol Stand* 1989; **70**: 27–47.
17 Niwa H, Yamamura K, Miyazaki J. Efficient selection for high-expression transfectants with a novel eukaryotic vector. *Gene* 1991; **108**: 193–199.
18 Takebe Y, Seiki M, Fujisawa J, Hoy P, Yokota K, Arai K *et al.* SRα promoter: an efficient and versatile mammalian cDNA expression system composed of the simian virus 40 early promoter and the R-U5 segment of the human T-cell leukemia virus type 1 long terminal repeat. *Mol Cell Biol* 1988; **8**: 466–472.
19 Tsurudome M, Kawano M, Yuasa T, Tabata N, Nishio M, Komada H *et al.* Identification of regions on the hemagglutinin-neuraminidase protein of human parainfluenza virus type 2 important for promoting cell fusion. *Virology* 1995; **213**: 190–203.
20 Tsurudome M, Nishio M, Komada H, Bando H, Ito Y. Extensive antigenic diversity among human parainfluenza type 2 virus isolates and immunological relationships among paramyxoviruses revealed by monoclonal antibodies. *Virology* 1989; **171**: 38–48.
21 Kawano M, Kaito M, Kozuka Y, Komada H, Noda N, Nanba K *et al.* Recovery of infectious human parainfluenza type 2 virus from cDNA clones and properties of the defective virus without V-specific cysteine-rich domain. *Virology* 2001; **284**: 99–112.
22 Calain P, Roux L. The rule of six, a basic feature for efficient replication of Sendai virus defective interfering RNA. *J Virol* 1993; **67**: 4822–4830.
23 Skiadopoulos MH, Vogel L, Riggs JM, Surman SR, Collins PL, Murphy BR. The genome length of human parainfluenza virus type 2 follows the rule of six, and recombinant viruses recovered from non-polyhexameric-length antigenomic cDNAs contain a biased distribution of correcting mutations. *J Virol* 2003; **77**: 270–279.
24 Tsurudome M, Nishio M, Ito M, Tanahashi S, Kawano M, Komada H *et al.* Effects of hemagglutinin-neuraminidase protein mutations on cell-cell fusion mediated by human parainfluenza type 2 virus. *J Virol* 2008; **82**: 8283–8295.
25 Tsurudome M, Ito M, Nishio M, Nakahashi M, Kawano M, Komada H *et al.* Identification of domains on the fusion (F) protein trimer that influence the hemagglutinin-neuraminidase specificity of the F protein in mediating cell–cell fusion. *J Virol* 2011; **85**: 3153–3161.
26 Palese P. RNA virus vectors: where are we and where do we need to go? *Proc Natl Acad Sci USA* 1998; **95**: 12750–12752.
27 Tao T, Skiadopoulos MH, Davoodi F, Surman SR, Collins PL, Murphy BR. Construction of a live-attenuated bivalent vaccine virus against human parainfluenza virus (PIV) types 1 and 2 using a recombinant PIV3 backbone. *Vaccine* 2001; **19**: 3620–3631.
28 Roberts A, Buonocore L, Price R, Forman J, Rose JK. Attenuated vesicular stomatitis viruses as vaccine vectors. *J Virol* 1999; **73**: 3723–3732.
29 Rose NF, Marx PA, Luckay A, Nixon DF, Moretto WJ, Donahoe SM *et al.* An effective AIDS vaccine based on live attenuated vesicular stomatitis virus recombinants. *Cell* 2001; **106**: 539–549.
30 Jones SM, Feldmann H, Ströher U, Geisbert JB, Fernando L, Grolla A *et al.* Live attenuated recombinant vaccine protects nonhuman primates against Ebola and Marburg viruses. *Nat Med* 2005; **11**: 786–790.
31 Kapadia SU, Rose JK, Lamirande E, Vogel L, Subbarao K, Roberts A. Long-term protection from SARS coronavirus infection conferred by a single immunization with an attenuated VSV-based vaccine. *Virology* 2005; **340**: 174–182.
32 Schwartz JA, Buonocore L, Roberts A, Suguitan A Jr, Kobasa D, Kobinger G *et al.* Vesicular stomatitis virus vectors expressing avian influenza H5 HA induce cross-neutralizing antibodies and long-term protection. *Virology* 2007; **366**: 166–173.
33 Lamb RA, Zebedee SL, Richardson CD. Influenza virus M2 protein is an integral membrane protein expressed on the infected-cell surface. *Cell* 1985; **40**: 627–633.
34 Sugrue RJ, Hay AJ. Structural characteristics of the M2 protein of influenza A viruses: evidence that it forms a tetrameric channel. *Virology* 1991; **180**: 617–624.
35 Shim BS, Choi YK, Yun CH, Lee EG, Jeon YS, Park SM *et al.* Sublingual immunization with M2-based vaccine induces broad protective immunity against influenza. *PLoS One* 2011; **6**: e27953.
36 Park KS, Lee J, Ahn SS, Byun Y-H, Seong BL, Baek YH *et al.* Mucosal immunity induced by adenovirus-based H5N1 HPAI vaccine confers protection against a lethal H5N2 avian influenza virus challenge. *Virology* 2009; **395**: 182–189.
37 Song K, Bolton DL, Wei C-J, Wilson RL, Camp JV, Bao S *et al.* Genetic immunization in the lung induces potent local and systemic immune responses. *Proc Natl Acad Sci USA* 2010; **107**: 22213–22218.
38 Le T-vL, Mironova E, Garcin D, Compans RW. Induction of influenza-specific mucosal immunity by an attenuated recombinant Sendai virus. *PLoS One* 2011; **6**: e18780.
39 Li HO, Zhu YF, Asakawa M, Kuma H, Hirata T, Ueda Y *et al.* A cytoplasmic RNA vector derived from nontransmissible Sendai virus with efficient gene transfer and expression. *J Virol* 2000; **74**: 6564–6569.
40 Kuypers J, Wright N, Ferrenberg J, Huang M-L, Cent A, Corey L *et al.* Comparison of real-time PCR assays with fluorescent-antibody assays for diagnosis of respiratory virus infections in children. *J Clin Microbiol* 2006; **44**: 2382–2388.
41 Nolan SM, Skiadopoulos MH, Bradley K, Kim OS, Bier S, Amaro-Carambot E *et al.* Recombinant human parainfluenza virus type 2 vaccine candidates containing a 3′ genomic promoter mutation and L polymerase mutations are attenuated and protective in non-human primates. *Vaccine* 2007; **25**: 6409–6422.

Microbiology and Immunology

Microbiol Immunol 2014; 58: 628–635
doi: 10.1111/1348-0421.12192

ORIGINAL ARTICLE

Ribavirin inhibits human parainfluenza virus type 2 replication *in vitro*

Sahoko Kihira[1], Jun Uematsu[2], Mitsuo Kawano[3], Ai Itoh[1], Ayumi Ookohchi[1], Saemi Satoh[1], Yurie Maeda[1], Kae Sakai[1], Hidetaka Yamamoto[4], Masato Tsurudome[3], Myles O'Brien[5] and Hiroshi Komada[2]

[1]Department of Clinical Nutrition, Faculty of Health Science, Suzuka University of Medical Science, [2]Microbiology and Immunology Section, Department of Clinical Nutrition, Graduate School of Suzuka University of Medical Science, 1001-1 Kishioka, Suzuka, Mie 510-0293, [3]Department of Microbiology, Mie University Graduate School of Medicine, 2-174 Edobashi, Tsu, Mie 514-8507, [4]Faculty of Pharmaceutical Science, Suzuka University of Medical Science, 3500-3 Minamitamagaki, Suzuka, Mie 513-8670 and [5]Graduate School of Mie Prefectural College of Nursing, 1-1-1 Yumegaoka, Tsu, Mie 514-0116, Japan

ABSTRACT

The antiviral activities of eight nucleoside analog antiviral drugs (ribavirin, acyclovir, lamivudine, 3′-azido-3′-deoxythymidine, emtricitabine, tenofovir, penciclovir and ganciclovir) against human parainfluenza virus type 2 (hPIV-2) were investigated. Only ribavirin (RBV) inhibited both cell fusion and hemadsorption induced by hPIV-2. RBV considerably reduced the number of viruses released from the cells. Virus genome synthesis was inhibited by RBV, as determined by real time PCR. An indirect immunofluorescence study showed that RBV largely inhibited viral protein synthesis. mRNAs of the proteins were not detected, indicating that inhibition of protein synthesis was caused by transcription inhibition by RBV. Using a recombinant green fluorescence protein-expressing hPIV-2 without matrix protein, it was found that RBV did not completely inhibit virus entry into the cells; however, it almost completely blocked multinucleated giant cell formation. RBV did not disrupt actin microfilaments and microtubules. These results indicate that the inhibitory effect of RBV is caused by inhibition of both virus genome and mRNA synthesis, resulting in inhibition of virus protein synthesis, viral replication and multinucleated giant cell formation (extensive cell-to-cell spreading of the virus).

Key words antiviral drugs, recombinant green fluorescence protein expressing hPIV-2 without matrix protein, human parainfluenza virus type 2.

Human parainfluenza virus type 2 is one of the major human respiratory tract pathogens of infants and children. hPIV-2, a member of the genus *Rubulavirus* in the family *Paramyxoviridae*, possesses a single-stranded, non-segmented, negative stranded RNA genome of 15,654 nucleotides (1). hPIV-2 has seven structural proteins, NP, V, P, M, F, HN and L proteins. The gene order of hPIV-2 is 3′-(leader)-NP-V/P-M-F-HN-L-(trailer)-5′. Our group has sequenced all genes of hPIV-2 (2–7). Tsurudome *et al.* made mAbs and investigated antigenic diversity of clinical isolates (8). Kawano *et al.* constructed infectious hPIV-2 from the cDNA clone and showed that its growth properties are the same as those of natural hPIV-2 (9).

Sahoko Kihira and Jun Uematsu contributed equally to this study.

Correspondence
Hiroshi Komada, Microbiology and Immunology Section, Department of Clinical Nutrition, Graduate School of Suzuka University of Medical Science, 1001-1 Kishioka, Suzuka, Mie 510-0293, Japan. Tel: +81 59 383 8991; fax: +81 59 383 9666; email: komada@suzuka-u.ac.jp

Received 9 March 2014; revised 4 August 2014; accepted 18 August 2014.

List of Abbreviations: AZT, 3′azido-3′-deoxythymidine; F, fusion; GFP, green fluorescence protein; Had, hemadsorption; HN, hemagglutininneuraminidase; hPIV-2, human parainfluenza virus type 2; L, large; M, matrix; NP, nucleoprotein; rhPIV-2ΔMGFP, a recombinant GFP-expressing hPIV-2 without matrix protein; P, phospho; RBV, ribavirin.

Ribavirin is a synthesized nucleoside analog that has broad antiviral activities against many DNA and RNA viruses. RBV in combination with IFN is reportedly an effective treatment for hepatitis C virus (10, 11) and respiratory syncytial virus (12). Its antiviral activity *in vitro* is mainly mediated by inhibition of inosine monophosphate dehydrogenase (13); however, the precise mechanism is still not fully understood.

In the present investigation, eight nucleoside analog drugs were tested for hPIV-2 growth: we found that only RBV has an inhibitory effect. To investigate the effect of the drugs on viral genome synthesis, we prepared and analyzed viral RNA by real time PCR. We synthesized cDNA using oligo dT primer and performed PCR to elucidate the effect of RBV on mRNA synthesis. We investigated virus protein expression by indirect immunofluorescence using mAbs against NP, F and HN proteins of hPIV-2 (8) and analyzed the inhibitory effects of RBV on hPIV-2 entry into the cells, and cell-to-cell spreading by using rhPIV-2ΔMGFP (14). We determined the number of viruses released from infected cells cultured with RBV. The cytoskeleton reportedly has an important role in paramyxovirus replication. Actin microfilaments are important in the hPIV-3 life cycle, specifically at the level of viral transport and replication (15). Tubulin also acts as a positive transcription factor for *in vitro* RNA synthesis by Sendai virus (16). We therefore analyzed the effects of RBV on actin microfilaments and microtubules using rhodamine phalloidin and anti-tubulin α mAb, respectively.

MATERALS AND METHODS

Antiviral drugs

Antiviral drugs, RBV, acyclovir, lamivudine, AZT, emtricitabine, tenofovir, penciclovir and ganciclovir were purchased from Wako Chemicals (Osaka, Japan). With the exception of penciclovir, they were dissolved at 1 mg/mL in 10 mM PBS, pH 7.2 (PBS), and sterilized by filtration. Penciclovir was dissolved at 1 mg/mL in dimethyl sulfoxide.

Virus and recombinant virus

The virus and recombinant virus were approved by the relevant biosafety committees of Suzuka University of Medical Science. hPIV-2 (Toshiba strain) was used. rhPIV-2ΔMGFP was constructed according to a previously described method (9, 17) and it was shown that it did not produce infectious virus particles without addition of M protein gene *in trans* (data not shown). Virus titers were determined using Vero cells. The virus yield was about 1×10^5 $TCID_{50}$/mL.

Cell line and cultivation of cells

$LLCMK_2$ cells (rhesus monkey kidney cell line) were cultured in flat-bottomed 24-well plates in 1 mL culture medium. Minimum essential medium-α (Wako, Osaka, Japan), supplemented with 2% FCS and 0.1 mg/mL kanamycin, was used. The cells were cultured at 37 °C in a humidified atmosphere with 5% CO_2. After 3 days, when the cells had become confluent (5×10^5 cells), the medium was changed to minimum essential medium-α with 0.5% FCS and 0.1 mg/mL kanamycin. The antiviral drugs were added to the cells, after which they were infected with hPIV-2 (3×10^2 $TCID_{50}$).

Cytopathogenic assay

Cell fusion and Had were observed at 4 days post-infection. The Had test was carried out by incubating the cells with 0.4% sheep red blood cells at room temperature for 30 min, washing four times with PBS and observing Had under a cell culture light microscope.

RNA preparation, cDNA synthesis and real time PCR

RNA was extracted from the cells (2×10^6 cells) cultured in flat-bottomed 6-well plates using TRIZOL reagent (Invitrogen, Carlsbad, CA, USA) according to the manufacturer's instructions. cDNA was synthesized with 1 μg RNA using Reverse Tra Ace qPCR RT Master Mix (Toyobo, Osaka, Japan) and NP gene specific primer (nucleotide number 1661–1679: 5′-CAACATTCAATGAATCAGT-3′). Real time PCR was performed on a ABI PRISM 7700 Sequence Detection System (Life Technologies, Tokyo, Japan) using TaqMan Probe (1932–1956: 5′-FAM-AAGCACCGGATTTCTAACCCGTCCG-TAMRA-3′), forward primer (1851–1875: 5′-ACACACTCATCCAGACAAATCAAAC-3′), and reverse primer (1958–1980: 5′-TGTGGAGGTTATCTGATCACGAA-3′).

Detection of messenger RNA (mRNA)

cDNA was synthesized with 1 μg RNA using oligo dT primer and superscript II reverse transcriptase (Invitrogen), and PCR performed with forward primers for NP (nucleotide number 1081–1100: 5′-CATGGCCAAGTACATGGCTC-3′), F (5821–5840: 5′-CCCTATCCCTGAATCACAAT-3′) and HN (7741–7760: 5′-ATTTCCTGTATATGGTGGTC-3′) genes of hPIV-2 (18), and reverse primers for NP (1,466–1489: 5′-CCTCCGAGTATCGATTGGATTGAA-3′), F (6661–6681: 5′-TGTCACGAGACGTTACGGACA-3′) and HN (8481–8500: 5′-GAACTCCCCTAAAAGAGATG-3′) genes and Ex Taq (Takara, Shiga, Japan).

Immunofluorescence studies

To detect virus proteins in the infected cells, the cells were fixed with 3.7% formaldehyde solution in PBS at room temperature for 15 min. The cells were then further incubated with 0.1% TritonX-100 in PBS at room temperature for 15 min to detect NP protein, which exists mainly in the cytoplasm, or for 3 min to detect F and HN proteins, which are in both the cytoplasm and the cell membrane. They were then washed with PBS and incubated with mouse mAbs against NP, F and HN proteins of hPIV-2 at room temperature for 30 min. After washing with PBS, the cells were incubated with Alexa 488 conjugated secondary antibody to mouse IgG (Invitrogen) at room temperature for 30 min, and observed under a fluorescence microscope (Olympus, Tokyo, Japan).

Actin was detected using rhodamine phalloidin (Invitrogen) and microtubules were observed using anti-tubulin α mAb against sea urchin tubulin α (clone B-5-1-2, Sigma-Aldrich, St Louis, MO, USA) at 20 hr of cultivation. The cells were fixed with 3.7% formaldehyde solution in PBS at 37 °C for 15 min, washed with PBS, then further incubated with 0.1% TritonX-100 in PBS at 37 °C for 3 min to detect actin and for 15 min to detect microtubules.

Entry and cell-to-cell spreading of hPIV-2

The drugs were added to the cells and, immediately after the addition, the cells were infected with rhPIV-2ΔMGFP (1×10^4 $TCID_{50}$), and cultured for 4 days. They were then fixed with 1.2% formaldehyde solution in PBS at room temperature for 15 min and observed under a fluorescence microscope.

RESULTS

Inhibitory effect of the eight antiviral drugs

Cell fusion and Had were observed at 4 days post-infection. RBV (10 and 20 μg/mL) had an inhibitory effect on cell fusion and Had (data not shown). The other seven drugs (20 μg/mL) showed no inhibitory effect on hPIV-2 replication. The eight antiviral drugs did not disturb normal cell morphology at the concentration used in the experiments.

In the subsequent experiments, RBV (20 μg/mL) and (as negative controls) acyclovir, lamivudine and AZT were used.

Titration of virus released from the infected cells

The titers of virus released from cells cultured with and without the drugs at 4 days post-infection were determined. Without the drugs, the virus titer was about 5×10^6 $TCID_{50}$/mL, whereas with RBV it was <10 $TCID_{50}$/mL, indicating that RBV had largely prevented viral replication and release of virus from the cells. Acyclovir, lamivudine and AZT had no effect on the number of viruses released from the cells.

Viral genome RNA synthesis

RNA was prepared from infected cells at 4 days post-infection and the viral genome RNA analyzed by real time PCR. Table 1 shows that RBV completely inhibited viral genome RNA and mRNA synthesis, whereas the other three antiviral drugs tested did not inhibit it. In the subsequent experiment, mRNA synthesis was analyzed. cDNA was synthesized using oligo dT primer and PCR performed using hPIV-2 specific primers for NP, F and HN genes. The number of base pairs between forward and reverse primers of NP, F and HN genes was about 400, 860 and 760, respectively. Figure 1 shows that NP (lane 4), F (lane 5) and HN (lane 6) mRNAs were detected in the virus-infected cells, but not in the RBV-treated infected cells (NP: lane 7, F: lane 8 and HN: lane 9), indicating that RBV inhibits transcription of viral genome. The other three antiviral drugs did not inhibit the synthesis of hPIV-2 mRNA (Fig. 1, lanes 10–18).

Viral protein synthesis

Indirect immunofluorescence study was performed to investigate the effects of the four selected antiviral drugs on hPIV-2 protein synthesis. The drugs were added to the cells, after which they were infected with hPIV-2. At 4 days post-infection, the cells were fixed and stained with mAbs against NP, F and HN proteins of hPIV-2.

Table 1. RBV inhibits hPIV-2 genome RNA synthesis

	Virus	RBV + virus	Acyclovir + virus	Lamivudine + virus	AZT + virus
No. of copies	635,463 ± 19,758	709 ± 55	740,196 ± 37,758	842,904 ± 22,841	790,270 ± 19,055

The numbers of viral genome copies were detected by real time PCR. Results are presented as mean ± SD of three experiments.